TOPOLOGY ERROR IDENTIFICATION WITH LIMITED NUMBER OF MEASUREMENTS IN POWER DISTRIBUTION SYSTEMS

A THESIS SUBMITTED TO
THE GRADUATE SCHOOL OF NATURAL AND APPLIED SCIENCES
OF
MIDDLE EAST TECHNICAL UNIVERSITY

BY

KEMAL PARLAKTUNA

IN PARTIAL FULFILLMENT OF THE REQUIREMENTS
FOR
THE DEGREE OF MASTER OF SCIENCE
IN
ELECTRICAL AND ELECTRONICS ENGINEERING

SEPTEMBER 2023

Approval of the thesis:

TOPOLOGY ERROR IDENTIFICATION WITH LIMITED NUMBER OF MEASUREMENTS IN POWER DISTRIBUTION SYSTEMS

submitted by **KEMAL PARLAKTUNA** in partial fulfillment of the requirements for the degree of **Master of Science in Electrical and Electronics Engineering Department, Middle East Technical University** by,

Prof. Dr. Halil Kalıpçılar
Dean, Graduate School of **Natural and Applied Sciences** _____

Prof. Dr. İlkay Ulusoy
Head of Department, **Electrical and Electronics Engineering** _____

Assoc. Prof. Dr. Murat Göl
Supervisor, **Electrical-Electronics Engineering, METU** _____

Examining Committee Members:

Prof. Dr. Ali Nezih Güven
Electrical-Electronics Engineering, METU _____

Assoc. Prof. Dr. Murat Göl
Electrical-Electronics Engineering, METU _____

Prof. Dr. Saffet Ayasun
Electrical-Electronics Engineering, Gazi University _____

Date:11.09.2023

I hereby declare that all information in this document has been obtained and presented in accordance with academic rules and ethical conduct. I also declare that, as required by these rules and conduct, I have fully cited and referenced all material and results that are not original to this work.

Name, Surname: Kemal Parlaktuna

Signature :

ABSTRACT

TOPOLOGY ERROR IDENTIFICATION WITH LIMITED NUMBER OF MEASUREMENTS IN POWER DISTRIBUTION SYSTEMS

Parlaktuna, Kemal
M.S., Department of Electrical and Electronics Engineering
Supervisor: Assoc. Prof. Dr. Murat Göl

September 2023, 65 pages

Electricity has become an indispensable part of the modern human. Traditionally electricity was generated, transmitted and distributed in different grid levels. Generation and distribution of electricity was not intertwined. Monitoring the distribution network was not necessary as the power was flowing unidirectionally and the loads were stationary, meaning that the distribution system operator had enough information to operate the system. However, with increasing popularity of renewable energy sources and mobile load technologies such as electric vehicles, the roles are not clearly defined for each grid level. These new advancements also bring new challenges and business opportunities for distribution system operator. The operator should improve its situational awareness on the system by conducting several analysis such as power flow or state estimation. Both of these methods rely on correct topology both in terms of parameters and switch statuses. Several switching actions occur daily in power distribution systems. Not all switches are equipped with communication devices that relay the current switch status. Even if the switches are equipped with communication devices, due to malfunctions or communication errors the known switch status might be different than the actual switch status. Moreover, state estimation also

requires redundant number of measurements which are not available in distribution level. Due to large system size in terms of bus number, not all elements of the system are equipped with both measurement instruments and devices to telemeter the gathered measurements. This thesis proposes a method for power distribution system with limited measurements to identify switch status mismatches using Direct Load Flow (DLF) and Weighted Least Absolute Values (WLAV) estimator.

Keywords: state estimation, direct load flow, situational awareness, distribution systems, topology identification

ÖZ

SINIRLI SAYIDA ÖLÇÜM BULUNAN GÜÇ DAĞITIM SİSTEMLERİNDE TOPOLOJİ HATASI TANILAMASI

Parlaktuna, Kemal
Yüksek Lisans, Elektrik ve Elektronik Mühendisliği Bölümü
Tez Yöneticisi: Doç. Dr. Murat Göl

Eylül 2023 , 65 sayfa

Elektrik enerjisi modern insan için vazgeçilmez olmuştur. Geleneksel olarak elektrik enerjisi üretim, iletim ve dağıtım olmak üzere farklı şebeke seviyelerinden oluşmaktaydı. Elektriğin üretimi ve dağıtımı iç içe değildi. Dağıtım şebekesi operatörü gücün tek yönlü akması ve yüklerin sabit olmasından dolayı şebekeyi detalı bir şekilde izlemeye gerek duymuyordu. Ancak, yenilenebilir enerji kaynaklarının popüleritelerinin artması ile elektrikli araçlar gibi mobil yüklerin sayısının artması, şebeke seviyelerinin rollerini de iç içe geçirdi. Bu yenilikler, operatör iş olanakları getirmesinin yanı sıra yeni zorluklar da getirerek operatörün durumsal farkındalığını arttırması zorunlu kıldı. Durumsal farkındalığı arttırmak için yük akış analizi ve durum kestirimi yapılması gerekmektedir. Bu analizleri yapabilmek için operatör hem parametreleri hem de kesici durumlarını tamamiyle doğru bildiği bir topoloji bilgisine ihtiyaç duymaktadır. Güç dağıtım sistemlerinde günlük olarak birçok kesici manevrası meydana gelmektedir. Ancak, bütün kesiciler durumlarını ileten bir iletişim cihazına sahip değildir. Sahip olsalar dahi iletişim hatalarından veya başka arızalardan dolayı doğru durum bilgisini aktaramayabilirler. Ayrıca zamanda doğru bir durum kestirim analizi yapa-

bilmek için sahada yeterli sayıda ölçüm bulunmalıdır. Bara sayısı bakımından büyük bir sistem boyutuna sahip olan dağıtım sistemlerinin bütün elemanlarında bir ölçüm cihazı bulunmamaktadır. Cihazın bulunduğu yerlerde ise her zaman iletişim cihazları bulunmamakta. Bu tez sınırlı sayıda ölçüm bulunan dağıtım sistemleri için kesici durumlarındaki uyumsuzlukları bulmak adına direkt yük analizi ve ağırlıklı en küçük mutlak değerler durum kestirim algoritmasını kullanan bir metod önermektedir.

Anahtar Kelimeler: durum kestirimi, direkt yük akışı analizi, durumsal farkındalık, dağıtım şebekesi, topoloji tanılaması

To my family.

ACKNOWLEDGMENTS

This work is funded by Scientific and Technological Research Council of Turkey (TUBİTAK) under BIDEB 2210-A funding.

I would like to express my gratitude to my supervisor Assoc. Prof. Murat Göl for his guidance, encouragement and criticism

I would like to thank Siemens A.Ş. especially Erk Dursun. Their insights on practical problems have been helpful during the development of this thesis.

I would like to thank my colleagues at Power System Analysis Laboratory whom I learned a lot through our discussions.

I would like to express my gratitude to Yaren Çayıroğlu and Kaan Kalaycıoğlu for their friendship over the years.

I would like to thank my wife and soul mate Ekin Tanır Parlaktuna for always cheering for me, lifting my spirit up and her invaluable support.

Lastly, I would like to thank my family. I could not achieve this degree without the support and love they showed.

TABLE OF CONTENTS

LIST OF TABLES

TABLES

LIST OF FIGURES

FIGURES

LIST OF ABBREVIATIONS

DSO	Distribution System Operator
PF	Power Flow
SE	State Estimation
SCADA	Supervisory Control and Data Acquisition
EMS	Energy Management System
WLS	Weighted Least Squares
FBPF	Forward-Backward Power Flow
DLF	Direct Load FLow
BIBC	Bus-Injection-to-Branch-Current
BCBV	Branch-Current-to-Bus-Voltage
LAV	Least Absolute Value
WLAV	Weighted Least Absolute Value
LP	Linear Programming
EMRA	Electricity Market Regulatory Authority
RTU	Remote Terminal Unit
RMSE	Root Mean Square Error
MAE	Mean Absolute Error
PMU	Phasor Measurement Unit
DC	Direct Current
BCSE	Branch Current Based State Estimation
NR	Newton-Raphson
GS	Gauss-Seidel
FDLF	Fast Decoupled Load Flow

CHAPTER 1

INTRODUCTION

Electricity has become an indispensable part of daily life. Traditionally electrical grid was composed of three main layers. These are generation level, transmission level and distribution level. These three layers had clearly defined roles where generation would happen mostly at generation level and commonly power would flow unidirectionally. Moreover, a significant daily change would not happen in loads. However, in modern distribution systems renewable energy source penetration has increased due to environmental concerns [1] and improvements in renewable energy production [2]. In addition, electric vehicles have become more accessible. Since these loads are mobile, bus loads may change drastically during the day based on driver behaviour. Summaries of traditional and modern power distribution grids are given respectively in Figure 1.1 and Figure 1.2.

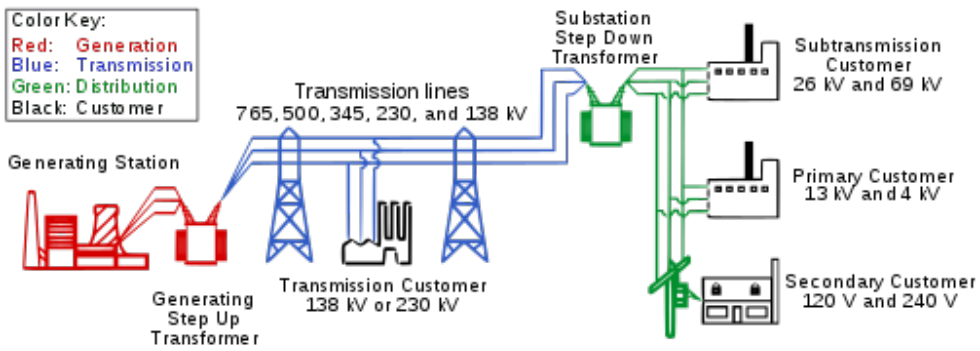

Figure 1.1: Traditional Power Grid

[https://3phaseassociates.com/basic-explanation-of-the-electric-power-grid/]

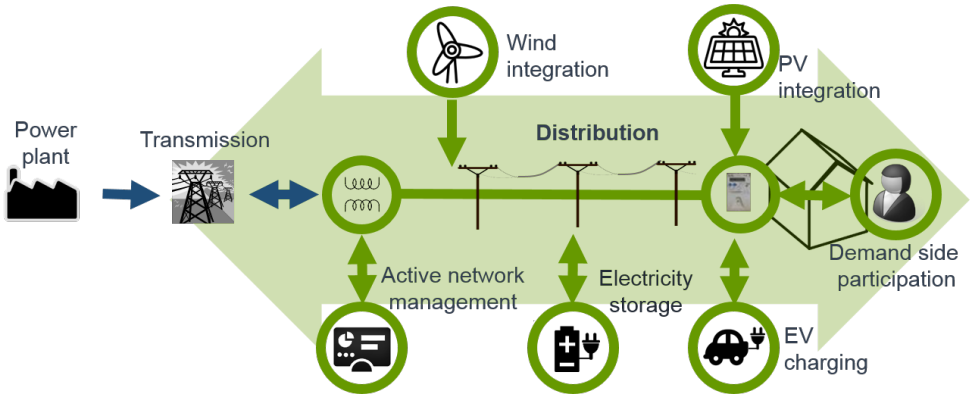

Figure 1.2: Modern Power Grid

[https://www.epfl.ch/labs/desl-pwrs/research/power-distribution-systems/]

Aforementioned changes and technological advancements have changed the operation of distribution systems. Distribution system operator (DSO) has to be aware of these changes and take actions accordingly as they can lead to unexpected conditions during operation. These unexpected conditions such as switching actions that DSO is unaware of may lead to dangerous situations for the field crew. Therefore, DSO has to improve its situational awareness of the system. In order to improve situational awareness the DSO uses several power system analysis tools such as power flow (PF) and state estimation (SE).

Although PF and SE have been comprehensively studied and are being applied in transmission level, distribution level has some research gaps and applications are limited. Distribution systems differ from the transmission network in the following aspects that affects the performance and applicability of such tools.

- Higher number of busses
- High R/X ratio
- Unbalanced loads
- Unbalanced topology
- Lack of transposition

- Lack of measurements

The unbalanced nature and high number of buses increase the size. Increasing size also increases the computational cost of any problem. Another problem is the lack of measurements which is crucial for state estimation. There may be thousands of buses in a distribution system where only a hundred of them are monitored with real-time measurements which means that system is not observable with real-time measurements. To overcome this problem, the methods proposed in this thesis utilize a common solution which is introducing pseudo power injection measurements. Pseudo power injection measurements are generally historical load consumption data, namely load profiles, that are available to DSO. Load profiles should be updated based on seasonal effects, such as increase in usage of air conditioning devices or heaters, and changes in customer behaviour.

1.1 Problem Definition

Power distributions systems are built in ring structures but are operated radially. Different types of configurations can be observed in Figure 1.3a, Figure 1.3b and Figure 1.3c. A bus can be connected to different transmission feeders at any given time depending on switch statuses as in Figure 1.3a. A bus can be connected to the same feeder through different paths depending on switch configurations as in Figure 1.3b. Or as in Figure 1.3c, the system can be radial. In reality, the system is composed of combinations of these configurations. Even though the system may operate meshed under short periods of time during switching actions, under normal operating conditions the system is operated radially. This means that if the branches where switches are closed are traced starting from any bus, no loops are encountered.

Precise topological information is crucial for energy management system (EMS) tools such as PF analysis and SE algorithms. Erroneous topological information leads incorrect analysis results, and incorrect results can mislead DSO to make false decisions and actions. These actions can be dangerous for distribution system operations. Erroneous topological information can be in the form of parameter errors. It can also be in the form of switch status error. Due to economical reasons not all switches are

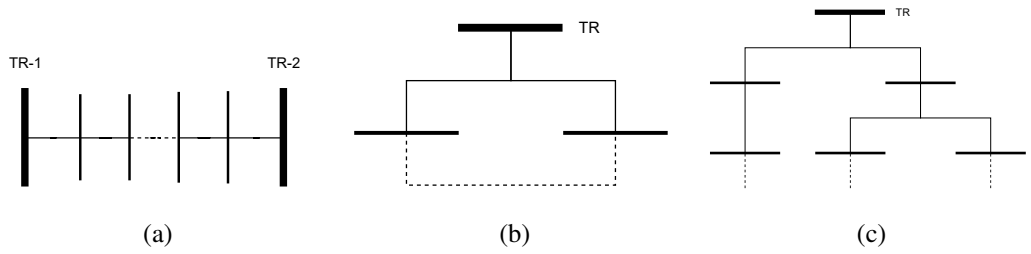

Figure 1.3: Various Power Distribution System Configurations

equipped with online switch status monitoring devices [3] in power distribution systems. Since the information is not carried online the operator may not know the exact switch statuses on the field any given time. This thesis proposes a weighted least absolute value (WLAV) SE based method to detect topological mismatches caused by switch status errors.

1.2 Literature Review

1.2.1 Topology Identification in Power Distribution Systems

Topological error identification is a well researched topic in observable systems. It was first recognized in [4]. Authors of [5] use normalized Lagrange multipliers to detect topology errors. In [6], direct current (DC) model of the system and mixed quadratic integer programming is utilized. Researchers also used state estimation to identify topology errors. In [7], authors use WLS problem to formulate the state estimation for topology error detection. In [8], a two-staged estimation along with LAV state estimation method is adopted for identification of unknown circuit breaker statuses.

However in distribution systems, not only the amount of data gathered is low compared to system size but the system is unobservable due to low number of measurements. In [9], branch current based state estimation (BCSE) which is a common practice for distribution system state estimation is used. To detect topology errors, authors change the on/off status of branches one by one and run BCSE. Then, if one of the cases results in a smaller residue compared to the residue of the original case, the

switch status from the field is considered false. Authors of [10] use a similar method where the most matching topology with state estimation results is chosen as correct. The computational time of these methods depend on the size of the system. With increasing system size, the switch count increases and so does the number of topology cases. This can be problematic for large distribution systems. Authors of [11] suggest a mixed integer nonlinear program to formulate the topology identification problem. The data used is based on μ-PMU's. These devices are not in widespread use and are not available for many distribution networks [12]. In another paper [13], authors use a method based on Markov Random Field to identify topology. They utilize both μ-PMUs and SCADA measurements.

1.2.2 Load Flow in Power Distribution Systems

Load flow is a well-studied subject in the literature, especially for transmission systems. The outcome of a load flow analysis is the voltage magnitudes and voltage angles at buses. The inputs to a load flow analysis are demands and generations of any given time and the precise system topology. Using these inputs calculations of every value in the system and violation detection is possible.

Various load flow methods are available in the literature, namely Newton-Raphson (NR), Gauss-Seidel (GS) and Fast-Decoupled-Load-Flow (FDLF) [14, 15]. GS is considered as the most simple one out of this three methods. The convergence is completely linear. However, the computational and the system size are proportional to each other. Increasing the system size decreases the convergence rate. The construction of Jacobian Matrix at every iteration of NR requires computational power but it has a quadratic type convergence [16]. Power distribution systems are mostly ill-conditioned power systems due to the features explained earlier and both NR and GS have known convergence issues due to the ill-conditioned system [17].

The distribution system is designed as open-ring where the radial path can change depending on switch statuses. The system is not operated in a meshed structure except rare transition cases. Using the radial structure, PF algorithm can be simplified. Forward-backward power flow (FBPF) is developed to be used with this property in mind [18]. A well-performing application of FBPF is direct load flow (DLF) which

is designed to work on radial and weakly meshed networks [19]. DLF is an iterative process where branch currents are calculated using bus voltages of the respective iteration. Then using the calculated branch currents, bus voltages of the next iteration are calculated. The process continues until a certain threshold for bus voltage changes is achieved.

1.2.3 State Estimation in Power Distribution Systems

SE problem in power systems is first recognized by Fred Schweppe [20–22]. Utilization of online SE has increased the capabilities of supervisory control and data acquisition (SCADA) introducing EMS. SCADA measurements, phasor measurement unit (PMU) measurements or a combination of both measurements are used for state estimation practices. In this study, SCADA measurements are taken into account as PMUs are seldomly installed at distribution level. The state estimator outputs are the most probable states of the system for a given measurement set. Common practice is to choose voltage magnitudes and voltage angles at each bus as system states. In this thesis, the system states are chosen as voltage magnitudes and voltage angles.

Various methods have been researched and applied for state estimation in power systems. Weighted least squares (WLS) SE is the most common method utilized in transmission system state estimation. However, its vulnerability to bad data can bias the estimator results significantly [23]. In power distribution networks, full system observability cannot be achieved using real-time measurements gathered from the field. A common method to achieve full observability is to use customer load profiles and forecasts to generate pseudo measurements. Reliability of such measurements depends on the performance of forecasts and the accuracy of load profiles. Even at the best case these measurements are unreliable compared to real-time measurements. A state estimator robust against bad data is crucial for obtaining accurate results when the unreliability of pseudo measurements is considered. Least absolute value (LAV) based state estimation rejects bad data as it uses the minimum number of confirming measurements that minimizes the error. Using WLAV further improves the performance as the weights of different measurements types can be adjusted according to reliability of the measurement.

1.3 Contribution of the Thesis

The contributions of this thesis are listed as follows:

- A systematic and automated analysis tool to detect topological mismatches in power distribution systems.
- A system reduction method to be used in power distribution system SE based on measurement locations.
- An algorithm to update consumer load profiles: Profiles are used for forecasts to generate pseudo measurements in systems with limited number of measurements to perform SE.
- An algorithm based on WLAV SE to detect topological mismatches in power distribution systems.

1.4 Structure of the Thesis

In this thesis, the work done is presented in four chapters. The structure is as follows:

The first chapter is the introduction where the problem definition and scope of this thesis are given. Moreover, the literature about the topic is reviewed. Research gaps in the literature and methods to address these gaps are highlighted.

In Chapter 2, theoretical background is established. Background information and mathematical formulations of DLF and WLAV are given. Pseudo-codes given in Appendix for DLF and WLAV are also mentioned.

In Chapter 3, proposed topological mismatch detection method is explained. The method is composed of three steps which are discussed under profile update, system reduction and topological mismatch detection sections. Methodology of DLF and WLAV are given in this chapter.

In Chapter 4, validation of the proposed method is given. In this chapter, methods are applied to a given network. Various test cases are generated from the network which are disclosed with figures.

Finally, in Chapter 5 the final remarks and the summary of the work done are given. Additionally, future works and improvements that can be made in the proposed method are indicated.

CHAPTER 2

BACKGROUND INFORMATION

In this chapter, the theoretical background for DLF and WLAV are given. The mathematical formulations for these tools are derived in detail. Pseudo-codes are presented at the end of each section.

2.1 Direct Load Flow

PF is an important anaylsis tool used to find system states for the current operating point of the system. Due to large system size and high R/X ratio in power distribution systems using common PF tools such as NR, GS or FDLF are not applicable. FBPF is a common method used for PF in power distribution networks. An application of FBPF is DLF. In DLF, the radial property of the distribution network is utilized for PF analysis. The most important advantage of DLF over the traditional FBPF is that the system is traversed once. After the traversal, system topology is saved in the form of two different matrices. However, in traditional FBPF system is traversed at each iteration, increasing computational burden.

Consider the radial distribution network with 6 buses given in Figure 2.1. The bus numbers are indicated in black while the branch numbers are indicated in red. The bus injection currents are indicated as $I_2 - I_6$. Bus number 1, connected to transmission network is selected as the slack bus and no load is located there ($I_1 = 0$). .

Using Equation 2.1, the bus injection currents can be found.

$$S = V \times I^* \tag{2.1}$$

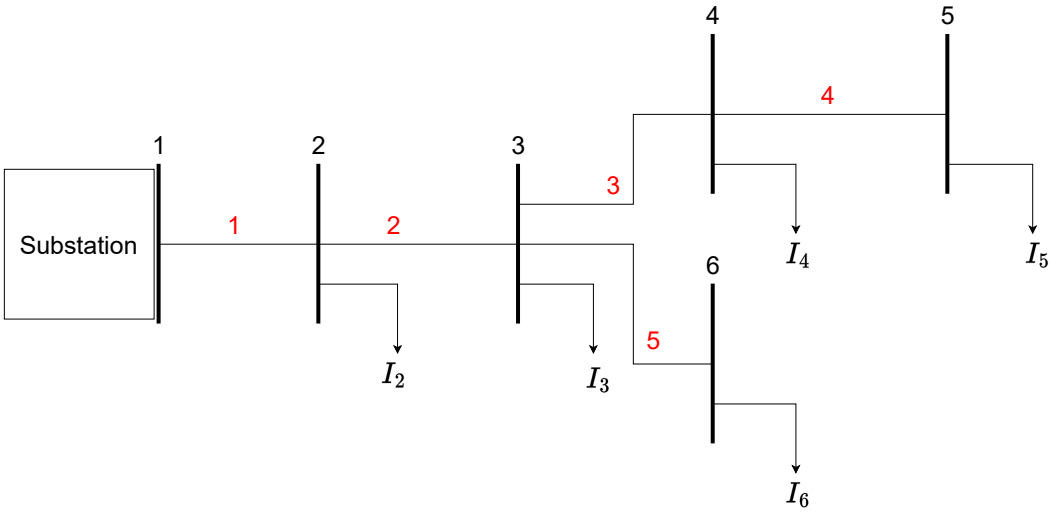

Figure 2.1: Simple 6 Bus Radial Distribution Network

Bus injection current vector, I_b, for the network given in Figure 2.1 can be observed in Equation 2.2. The initial voltages, where k=1, are selected equal to bus 1 (slack bus).

$$I_b^{[k]} = \left[\left(\frac{S_2}{V_2^{[k]}}\right)^*, \left(\frac{S_3}{V_3^{[k]}}\right)^*, \left(\frac{S_4}{V_4^{[k]}}\right)^*, \left(\frac{S_5}{V_5^{[k]}}\right)^*, \left(\frac{S_6}{V_6^{[k]}}\right)^* \right]^T \tag{2.2}$$

Where:

k : iteration number

V_i^k : voltage at i$^{\text{th}}$ bus for k$^{\text{th}}$ iteration

S_i : complex power demand of i$^{\text{th}}$ bus

Radial configuration of the system allows branch currents to be written in terms of bus injection currents. For example, the current at branch 5 can be expressed in terms bus injection current at bus 6. Likewise, the current at branch 3 can be expressed in terms of injection currents of buses 4 and 5. Applying the same methodology, every branch current can be written in terms of bus injection currents. It is possible to express the formulation in matrix form, namely the bus injection to branch current (BIBC) matrix. The BIBC matrix of the system in Figure 2.1 is given in Equation 2.3. The rows of BIBC matrix represent the branch number and the columns represent the

buses.

$$BIBC = \begin{bmatrix} 1 & 1 & 1 & 1 & 1 \\ 0 & 1 & 1 & 1 & 1 \\ 0 & 0 & 1 & 1 & 0 \\ 0 & 0 & 0 & 1 & 0 \\ 0 & 0 & 0 & 0 & 1 \end{bmatrix} \tag{2.3}$$

Please note that cable shunt capacitances or compensation units connected to buses contribute to branch currents. The shunt element current vector, I_s, for the system in Figure 2.1 can be calculated using Equation 2.4.

$$I_s^{[k]} = \begin{bmatrix} Y_{2,s} \\ Y_{3,s} \\ Y_{4,s} \\ Y_{5,s} \\ Y_{6,s} \end{bmatrix} \times \left[V_2^{[k]}, V_3^{[k]}, V_4^{[k]}, V_5^{[k]}, V_6^{[k]} \right] \tag{2.4}$$

Where:

k : iteration number

V_i^k : voltage at i$^{\text{th}}$ bus for k$^{\text{th}}$ iteration

$Y_{i,s}$: shunt admittance connected to i$^{\text{th}}$ bus

Branch currents can be expressed as in Equation 2.5.

$$I^{[k]} = BIBC \times I_b^{[k]} + I_s^{[k]} \tag{2.5}$$

The relationship between branch currents and voltage change across branches is expressed using branch current to bus voltage (BCBV) matrix. Again, consider the system in Figure 2.1. If bus 1 is chosen as the slack bus, the voltage at bus 2 can be expressed by the current flowing through and the impedance of branch 1 as well as the voltage at bus 1. Similarly, the voltage at bus 4 can be expressed by currents flowing and impedances at branches 1, 2 and 3 as well as the voltage at bus 1. The

BCBV matrix for the system in Figure 2.1 is given in Equation 2.6.

$$BCBV = \begin{bmatrix} Z_1 & 0 & 0 & 0 & 0 \\ Z_1 & Z_2 & 0 & 0 & 0 \\ Z_1 & Z_2 & Z_3 & 0 & 0 \\ Z_1 & Z_2 & Z_3 & Z_4 & 0 \\ Z_1 & Z_2 & 0 & 0 & Z_5 \end{bmatrix} \tag{2.6}$$

Where:

Z_i : impedance of i$^{\text{th}}$ branch

As it can be observed in Equation 2.7, multiplication branch current vector, $I^{[k]}$ and BCBV matrix reveals the voltage differences between the slack bus and other buses. The initial bus voltages are set as the slack bus voltage.

$$\Delta V^{[k]} = \begin{bmatrix} \Delta V_2^{[k]} \\ \Delta V_3^{[k]} \\ \Delta V_4^{[k]} \\ \Delta V_5^{[k]} \\ \Delta V_6^{[k]} \end{bmatrix} = \begin{bmatrix} V_1 - V_2^{[k]} \\ V_1 - V_3^{[k]} \\ V_1 - V_4^{[k]} \\ V_1 - V_5^{[k]} \\ V_1 - V_6^{[k]} \end{bmatrix} = BCBV * I^{[k]} \tag{2.7}$$

Where:

V_1 : set voltage at bus 1 (slack bus)

$V_i^{[k]}$: voltage at i$^{\text{th}}$ bus at k$^{\text{th}}$ iteration

$\Delta V_i^{[k]}$: difference between i$^{\text{th}}$ bus voltage and slack bus voltage at k$^{\text{th}}$ iteration

$\Delta V^{[k]}$: voltage change vector for iteration k

The voltages are updated at each iteration using the voltage change vector, $\Delta V^{[k]}$, and the respective equation is given in Equation 2.8.

$$V^{[k+1]} = V_1 - \Delta V^{[k]} \tag{2.8}$$

The iterations continue until a convergence is achieved, where the maximum value of voltage magnitudes is less than a set threshold value. The convergence criteria is given in Equation 2.9

$$V^{[k+1]} - V^{[k]} < \epsilon \tag{2.9}$$

The DLF algorithm is given in Appendix A Algorithm 1.

2.2 Weighted-Least Absolute Value (WLAV) Estimation

State estimation is crucial for all EMS. The estimator obtains the system states, namely the bus voltage magnitudes and bus voltage phase angles. WLAV estimation is an extension to commonly used LAV estimation. The weights of different types of measurements are adjusted based on their reliability. Higher weights result in smaller residuals. Hence if a measurement type is trusted more, its weight is also higher compared to other measurements. Using LAV estimator without adjusting the weights would yield a biased result towards pseudo measurements. Using WLS estimator would result in problems against bad data as WLS estimator is not a robust estimator vs bad data. With low measurement redundancy, running a bad data analysis to remove measurements with bad data is not desirable in distribution systems with limited measurements.

There are certain assumptions made for SE. The system is assumed to be balanced in terms of power and it operates at steady state. Hence, all components and states are modeled using positive-sequence model. Another assumption is that the measurement errors are independent, i.e., $E\{e_i e_j\} = 0$. The measurements are collected by SCADA or PMU. In this thesis, measurements are considered to be taken from SCADA. Measurement model of the estimator can be observed in Equation 2.10.

$$z = \begin{bmatrix} z_1 \\ z_2 \\ \vdots \\ z_m \end{bmatrix} = \begin{bmatrix} h_1(x_1, x_2, \ldots, x_n) \\ h_2(x_1, x_2, \ldots, x_n) \\ \vdots \\ h_m(x_1, x_2, \ldots, x_n) \end{bmatrix} + \begin{bmatrix} e_1 \\ e_2 \\ \vdots \\ e_m \end{bmatrix} = h(x) + e \tag{2.10}$$

Where:

$h_i(x)$: non-linear function that relates measurements i to the state vector x

z : measurement set ($m \times 1$)

e : measurement error vector ($m \times 1$)

x : system state vector ($n \times 1$)

m : number of measurements

n : number of states

Consider the objective function of LAV SE given in Equation 2.11 .

$$\begin{aligned} \min \quad & \sum_{i=1}^{m} |c_i r_i| \\ \text{s.t.} \quad & z_i = h_i(x) + r_i,\ 1 \leq i \leq m \end{aligned} \tag{2.11}$$

Where:

r_i : is the measurement residual, i.e., the difference i[th] measurement and the estimated value of that measurement

c_i : is the measurement weight of i[th] measurement

The measurement residual, r_i, is defined as the difference between the i[th] measurement and the estimated value of the measurement. Assuming that x^0 is the initial solution of the problem, the first-order approximation of the measurement function $h(x)$ around x^0 can be solved using a set of linear programming (LP) problems. Reorganizing the objective function inEquation 2.11, the expression in Equation 2.12 can be obtained.

$$\begin{aligned} \min \quad & \sum_{i=1}^{m} (u_i^k + v_i^k) \\ \text{s.t.} \quad & H \cdot \Delta x_u - H \cdot \Delta x_v + u - v = \Delta z \\ & \Delta x_u, \Delta x_v, u, v \geq 0 \end{aligned} \tag{2.12}$$

Where:

Δx = $\Delta x_u - \Delta x_v$

$u_i^k - v_i^k$ = $z - h(x^k) - H(x^k) \cdot \Delta x$

$h_i(x)$: non-linear function that relates measurement i to the state vector x

z : measurement set ($m \times 1$)

e : measurement error vector ($m \times 1$)

x : system state vector ($n \times 1$)

m : number of measurements

n : number of states

Writing the problem in standard LP problem format we obtain Equation 2.13.

$$\begin{aligned} \min \quad & c^T \cdot Y \\ \text{s.t.} \quad & A \cdot Y = b \\ & Y \geq 0 \end{aligned} \tag{2.13}$$

Where:

c^T = $\left[0_n, 0_n, c_m, c_m\right]$

0_n : vector of zeros of size ($n \times 1$)

c_m : cost vector of size ($m \times 1$)

b = Δz

Y^T = $\left[\Delta x_u^T, \Delta x_v^T, u^T, v^T\right]$

A = $\left[H, -H, I_m, -I_m\right]$

I_m : identity matrix of size ($m \times 1$)

H : measurement Jacobian Matrix

Simplex based optimization algorithm is utilized to solve for problem given in Equation 2.13. At each iteration, $|\Delta X|$ is checked. When it is lower than a predefined threshold, the solution of the algorithm is revealed. The measurement Jacobian matrix, H, is derived from the measurement function, $h(x^k)$. The measurement functions

for power injections, power flows and current magnitudes are given in Equation 2.14 - Equation 2.18.

$$P_i = V_i \cdot \sum_{j \in N_i} V_j \cdot (G_{ij} \cos\theta_{ij} + B_{ij} \sin\theta_{ij}) \tag{2.14}$$

$$Q_i = V_i \cdot \sum_{j \in N_i} V_j \cdot (G_{ij} \sin\theta_{ij} - B_{ij} \cos\theta_{ij}) \tag{2.15}$$

$$P_{ij} = V_i^2 \cdot (g_{si} + g_{ij}) - V_i \cdot V_j \cdot (g_{ij} \cdot \cos\theta_{ij} + b_{ij} \sin\theta_{ij}) \tag{2.16}$$

$$Q_{ij} = -V_i^2 \cdot (b_{si} + b_{ij}) - V_i \cdot V_j \cdot (g_{ij} \cdot \sin\theta_{ij} - b_{ij} \cos\theta_{ij}) \tag{2.17}$$

$$|I_{ij}| = \sqrt{(g_{ij}^2 + b_{ij}^2)(V_i^2 + V_j^2 - 2V_iV_j \cos\theta_{ij})} \tag{2.18}$$

Where:

V_i, θ_i	: magnitude and angle of the voltage phasor at bus i
θ_{ij}	: angle difference between bus i and bus j ($\theta_i - \theta_j$)
$G_{ij} + jB_{ij}$	: ij$^{\text{th}}$ element of the bus admittance matrix
$g_{ij} + jb_{ij}$	: series admittance of the branch connecting bus i and bus j
$g_{si} + jb_{si}$	: shunt admittance of the branch connected to bus i
N_i	: set of buses that are connected to bus i

As mentioned, Jacobian matrix, H, is derived from the measurement function, $h(x^k)$, by taking the partial derivatives of equations given in Equation 2.14 - Equation 2.18 and the voltage magnitude measurements with respect to system states. The general structure of the H matrix can be observed in Equation 2.19.

$$H = \begin{bmatrix} 0 & \frac{\partial V_{mag}}{\partial V} \\ \frac{\partial P_i}{\partial \theta} & \frac{\partial P_i}{\partial V} \\ \frac{\partial Q_i}{\partial \theta} & \frac{\partial Q_i}{\partial V} \\ \frac{\partial P_{ij}}{\partial \theta} & \frac{\partial P_{ij}}{\partial V} \\ \frac{\partial Q_{ij}}{\partial \theta} & \frac{\partial Q_{ij}}{\partial V} \\ \frac{\partial |I_{ij}|}{\partial \theta} & \frac{\partial |I_{ij}|}{\partial V} \end{bmatrix} \tag{2.19}$$

The H matrix is a $(m \times (2n-1))$ matrix where the rows represent the measurements

and the columns represent the system states. There are $(2n-1)$ system states as the slack bus angle is known. Formulation for each element of H matrix is given explicitly in Equation 2.20 - Equation 2.25.

- Voltage magnitude measurement elements:

$$\begin{aligned}
\frac{\partial V_i}{\partial \theta_i} &= 0 \\
\frac{\partial V_i}{\partial V_j} &= 0 \\
\frac{\partial V_i}{\partial V_i} &= 1 \\
\frac{\partial V_i}{\partial V_j} &= 0
\end{aligned} \tag{2.20}$$

- Real power injection measurement elements:

$$\begin{aligned}
\frac{\partial P_i}{\partial \theta_i} &= \sum_{j=1}^{N} V_i V_j(-G_{ij}\sin\theta_{ij} + B_{ij}\cos\theta_{ij}) - V_i^2 B_{ii} \\
\frac{\partial P_i}{\partial \theta_j} &= V_i V_j(G_{ij}\sin\theta_{ij} - B_{ij}\cos\theta_{ij}) \\
\frac{\partial P_i}{\partial V_i} &= \sum_{j=1}^{N} V_j(G_{ij}\cos\theta_{ij} + B_{ij}\sin\theta_{ij}) + V_i G_{ii} \\
\frac{\partial P_i}{\partial V_j} &= V_i(G_{ij}\cos\theta_{ij} + B_{ij}\sin\theta_{ij})
\end{aligned} \tag{2.21}$$

- Reactive power injection measurement elements:

$$\begin{aligned}
\frac{\partial Q_i}{\partial \theta_i} &= \sum_{j=1}^{N} V_i V_j(G_{ij}\cos\theta_{ij} + B_{ij}\, in\theta_{ij}) - V_i^2 G_{ii} \\
\frac{\partial Q_i}{\partial \theta_j} &= V_i V_j(-G_{ij}\cos\theta_{ij} - B_{ij}\sin\theta_{ij}) \\
\frac{\partial Q_i}{\partial V_i} &= \sum_{j=1}^{N} V_j(G_{ij}\sin\theta_{ij} - B_{ij}\cos\theta_{ij}) - V_i B_{ii} \\
\frac{\partial Q_i}{\partial V_j} &= V_i(G_{ij}\sin\theta_{ij} - B_{ij}\cos\theta_{ij})
\end{aligned} \tag{2.22}$$

- Real power flow measurement elements:

$$\begin{aligned}
\frac{\partial P_{ij}}{\partial \theta_i} &= V_i V_j (g_{ij} \sin\theta_{ij} - b_{ij} \cos\theta_{ij}) \\
\frac{\partial P_{ij}}{\partial \theta_j} &= -V_i V_j (g_{ij} \sin\theta_{ij} - b_{ij} \cos\theta_{ij}) \\
\frac{\partial P_{ij}}{\partial V_i} &= -V_j (g_{ij} \cos\theta_{ij} + b_{ij} \sin\theta_{ij}) + 2(g_{ij} + g_{si}) V_i \\
\frac{\partial P_{ij}}{\partial V_j} &= -V_i (g_{ij} \cos\theta_{ij} + b_{ij} \sin\theta_{ij})
\end{aligned} \tag{2.23}$$

- Reactive power flow measurement elements:

$$\begin{aligned}
\frac{\partial Q_{ij}}{\partial \theta_i} &= -V_i V_j (g_{ij} \cos\theta_{ij} + b_{ij} \sin\theta_{ij}) \\
\frac{\partial Q_{ij}}{\partial \theta_j} &= V_i V_j (g_{ij} \cos\theta_{ij} + b_{ij} \sin\theta_{ij}) \\
\frac{\partial Q_{ij}}{\partial V_i} &= -V_j (g_{ij} \sin\theta_{ij} - b_{ij} \cos\theta_{ij}) - 2V_i (b_{ij} + b_{si}) \\
\frac{\partial Q_{ij}}{\partial V_j} &= -V_i (g_{ij} \sin\theta_{ij} - b_{ij} \cos\theta_{ij})
\end{aligned} \tag{2.24}$$

- Current magnitude measurement elements, where shunt admittance of the branch is ignored:

$$\begin{aligned}
\frac{\partial |I_{ij}|}{\partial \theta_i} &= \frac{g_{ij}^2 + b_{ij}^2}{|I_{ij}|} V_i V_j \sin\theta_{ij} \\
\frac{\partial |I_{ij}|}{\partial \theta_j} &= -\frac{g_{ij}^2 + b_{ij}^2}{|I_{ij}|} V_i V_j \sin\theta_{ij} \\
\frac{\partial |I_{ij}|}{\partial V_i} &= -\frac{g_{ij}^2 + b_{ij}^2}{|I_{ij}|} (V_i - V_j \cos\theta_{ij}) \\
\frac{\partial |I_{ij}|}{\partial V_i} &= -\frac{g_{ij}^2 + b_{ij}^2}{|I_{ij}|} (V_j - V_i \cos\theta_{ij})
\end{aligned} \tag{2.25}$$

The WLAV SE algorithm is given in Appendix A Algorithm 2.

2.3 Chapter Summary

In this chapter, the theoretical background as well as the mathematical derivation are explained. In Section 2.1 DLF method is explained in detail, while in Section 2.2 WLAV SE method is clarified. Pseudo-codes for both methods can also be observed

in Appendix A. In the following chapter the proposed method will be explained, where DLF is utilized to validate the results of customer load profile update method. WLAV SE is used to reveal states both at updated profile method and at topological mismatch detection procedure.

CHAPTER 3

PROPOSED METHOD

In this chapter, the proposed method for topological mismatch identification is explained. The proposed method is composed of three steps.

First since there are limited number of telemetered measurements, the distribution system is not observable. In order to increase the number of measurements and achieve full system observability, pseudo measurements are introduced. Accuracy of such data is low as they are based on forecasts. With growing cities, the energy demand also changes. It not only increases but can also decrease due to newly installed renewable energy sources. Hence, to improve detection performance and reduce the uncertainties caused by pseudo measurements, customer load profiles that are generating pseudo measurements have to be updated regularly.

Second, after updating the profiles, a system reduction is performed. Around 10-20% of distribution system buses are equipped with measurement devices and remote terminal units (RTUs) at most. The pseudo measurements at buses not equipped with measurement instruments or RTUs become critical measurements. A system reduction based on real-time measurement locations is performed.

Lastly, a WLAV SE is run for the given measurement set and the reduced topology. A post-process where the results are interpreted is conducted.

Assumptions for the proposed method are as follows:

1. Real-time measurements do not carry bad data.
2. Measurement instruments are considered to be connected in correct polarization.

3. If a bus has large enough renewable energy sources to make that bus active, it is equipped with measurement instruments and the measurements are telemetered.

All three steps of the proposed method are explained in the following subsections.

3.1 Profile Update

Load profiles are hourly average load demands of the customer. These profiles are available to the system operator. They change due to seasonal effects or customer behaviour and should be updated regularly. Examples of customer load profiles are shown in Figure 3.1.

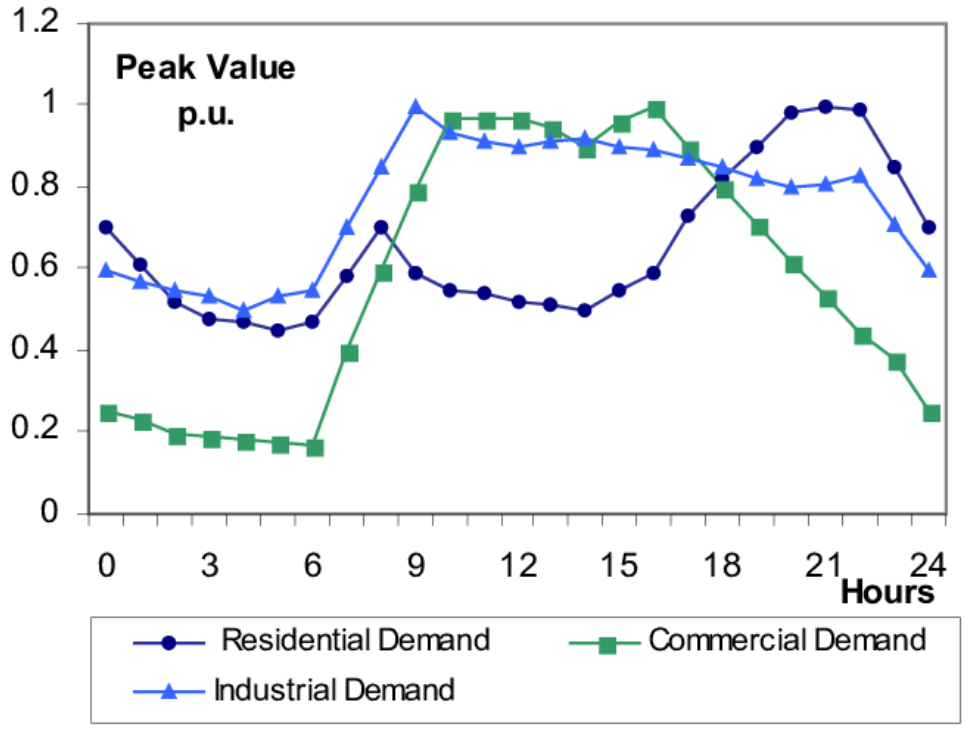

Figure 3.1: Various Customer Load Profile Examples

[https://www.researchgate.net/figure/Demand-curve-for-the-residential-industrial-and-commercial-loads_fig3_3266841]

The proposed profile update method utilizes both WLAV and DLF. The low measurement redundancy of distribution systems is compensated using load profiles as pseudo measurements. The WLAV estimator finds the true states of the system as close as possible. Please note that the reliability of the results depends on the number of real-time measurements. Pseudo measurements where a substantial difference between the original measurement values and the values calculated with WLAV results are updated with Equation 2.14 and Equation 2.15,

The flowchart of the proposed method can be observed in Figure 3.2.

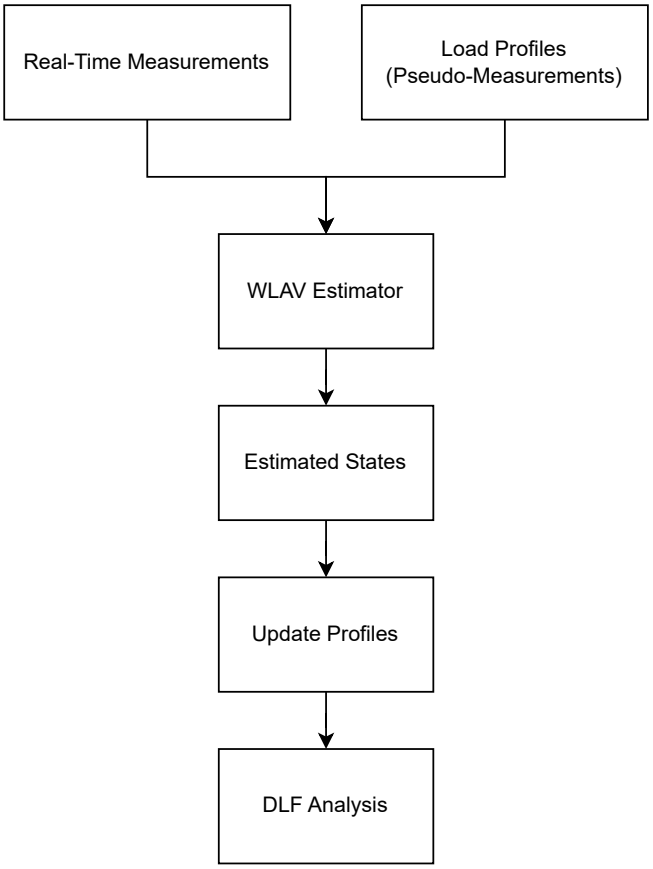

Figure 3.2: Flowchart of Profile Update Method

Note that for customer load profiles to be updated the precise topology information is required. DSO should update profiles using this method only when the operator is sure that the topology is correct.

3.2 Reduction Procedure

Full system observability is achieved using pseudo measurements based on historical data. Since the only measurements at certain parts of the system are pseudo measurements, they become critical measurements and bias SE results. To prevent biasing, a system reduction based on telemetered measurement location is proposed. First, the name convention for the method and the measurement configuration is explained. After that, the reduction procedure is explained with an example.

3.2.1 Name Convention and Measurement Configuration

The number of real-time measurements are limited in power distribution system because not all buses are equipped with real-time measurement devices. Even if a bus is equipped with measuring instruments, they may not be equipped with RTUs that telemeter these measurements. The buses can fall into three categories based on measurement device availability, observability and number of connections to buses with measurement devices. In terms of measurement device availability, buses equipped with both real-time measurement instruments and RTUs are called telemetered buses, while the rest of the buses fall into non-telemetered bus category. In terms of observability, buses that are observable with real-time measurements are called observable buses and the rest are called unobservable buses. Lastly, a bus is called an intersection bus if it has more than three branches connected and the branches lead to a telemetered bus. A bus can be in multiple groups. To further clarify the bus types, consider the distribution network given in Figure 3.3 and the types given in Table 3.1. The dashed line between bus 12 and bus 20 indicates an open switch. The buses highlighted with color red are telemetered buses and the connection to transmission level is shown with an arrow at bus 0.

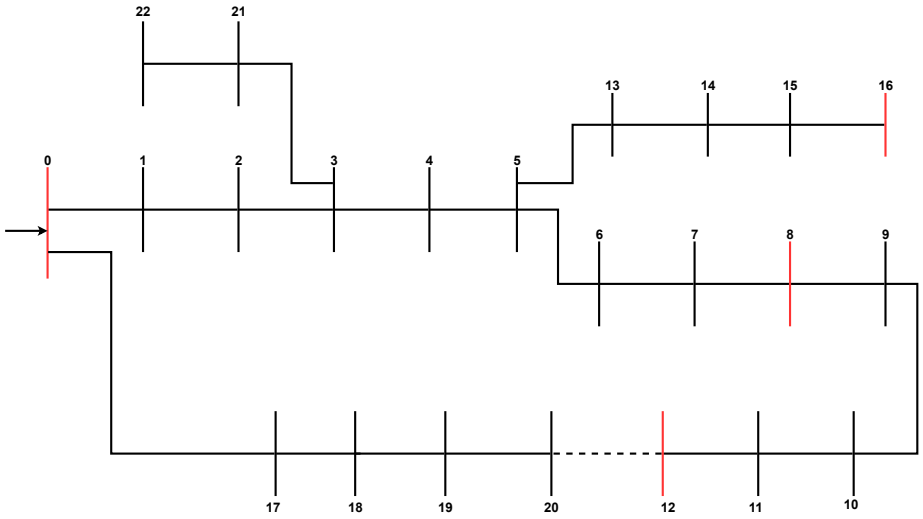

Figure 3.3: Example Power Distribution System

Table 3.1: Bus Types

Bus	Type	Number	Type	Bus	Type	Bus	Type
0	T-O	6	NT-U	12	T-O	18	NT-U
1	NT-O	7	NT-O	13	NT-U	19	NT-U
2	NT-U	8	T-O	14	NT-U	20	NT-U
3	NT-U	9	NT-O	15	NT-O	21	NT-U
4	NT-U	10	NT-U	16	T-O	22	NT-U
5	NT-U-I	11	NT-O	17	NT-O		

T : Telemetered Buses NT : Non-Telemetered Buses

O : Observable Buses U : Unobservable Buses

I : Intersection Buses

Since branch 3-21 that is connected to bus 3 is not leading to a telemetered bus, bus number 3 is not an intersection. However, all branches connected to bus 5 lead to a telemetered bus, making bus number 5 an intersection bus.

All measurement types are assumed to be available at telemetered buses. These are power injections at buses, power flows at branches, current magnitudes of branches,

which are given in Equation 2.14 - Equation 2.18 and voltage magnitude measurements at buses. No real-time measurements are gathered from non-telemetered buses. Parts of the system are not observable with real-time measurements and pseudo measurements, based on forecasts and historical data, are introduced for non-telemetered buses.

3.2.2 System Reduction

System reduction is a procedure to reduce system size. The size is reduced based on real-time measurement locations. The aim is to remove the number of pseudo measurements that are critical measurements so that the system is not biased.

Pseudo measurements at unobservable and non-telemetered buses are critical measurements. Since pseudo measurements do not reflect the current status of the system, they bias the SE result. The proposed method relies on reduction of the network based on telemetered bus locations. Consider the distribution network given in Figure 3.3. Pseudo measurements are introduced for all non-telemetered buses. Pseudo measurements of unobservable buses are added to observable buses. The addition can be to either one of the observable bus as there are no real-time measurements at the branches between non-telemetered buses that would be affected. The intersection buses are kept the same. The branches between two non-telemetered unobservable buses that remain between two telemetered buses when traced are connected in series. The procedure of adding pseudo measurements and connecting series branches will be named as merging from now on. The reduction procedure is as follows:

1. Merge radial connected leaf nodes until a non-telemetered observable bus or a bus with more than three branches connected is reached.
2. Check for new non-telemetered unobservable leaf buses. If it exists, go to the first step. If it does not exist, go to the next step.
3. Merge non-telemetered unobservable buses that are not intersections to non-telemetered observable buses.

The reduction procedure flowchart is given in Figure 3.4.

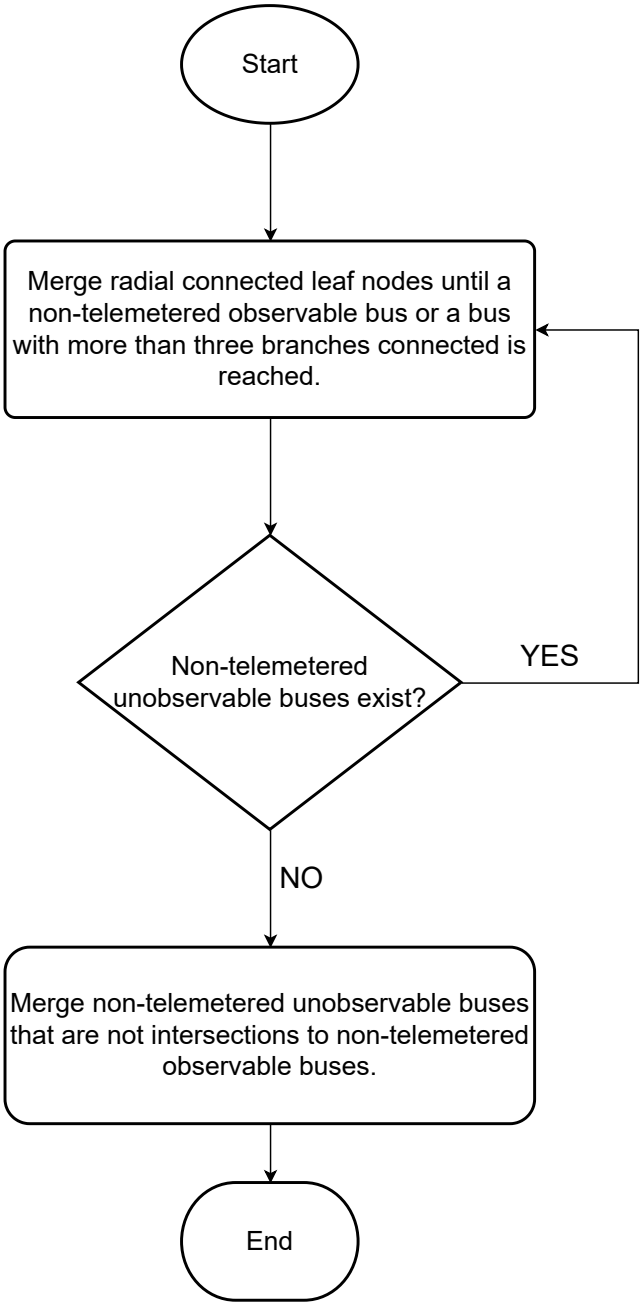

Figure 3.4: Reduction Procedure Flowchart

The reduced networks for the system in Figure 3.3 after step 1 and step 3 can be observed in Figure 3.5 and in Figure 3.6, respectively.

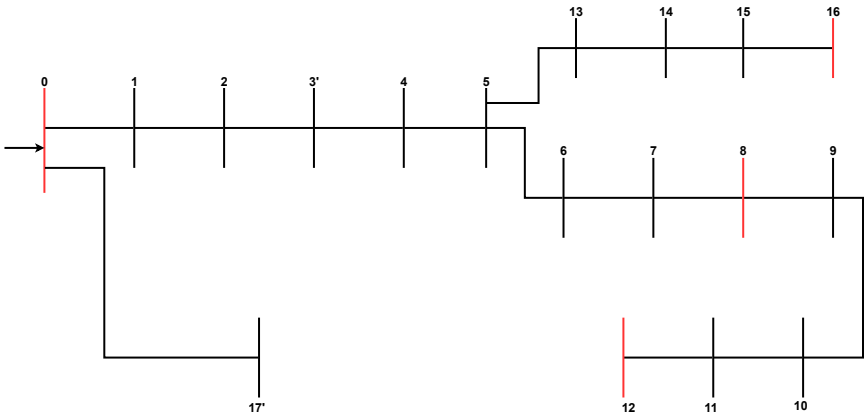

Figure 3.5: Reduced Network After Step 1

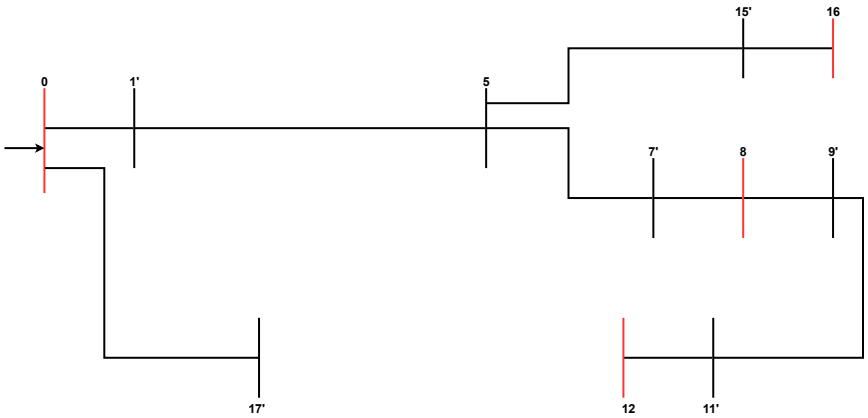

Figure 3.6: Reduced Network After Step 2

The reduced network pseudo measurements and their compositions are shown in Table 3.2 and Table 3.3.

Table 3.2: Bus Composition of Reduced System

Reduced Bus	Bus Composition	Reduced Bus	Bus Composition
$1'$	1, 2, 3, 4, 21, 22	$11'$	11
$5'$	5	$15'$	13,14,15
$7'$	6, 7	$17'$	17, 18, 19, 20
$9'$	9, 10		

Table 3.3: Branch Composition of Reduced System

Reduced Branch	Branch Composition	Reduced Branch	Branch Composition
$0'$-$1'$	0-1	$8'$-$9'$	8-9
$0'$-$17'$	0-17	$9'$-$11'$	9-10, 10-11
$1'$-5	1-2, 2-3, 3-4, 4-5	$11'$-$12'$	11-12
5-$7'$	5-6, 6-7	$5'$-$15'$	5-13, 13-14, 14-15
$7'$-$8'$	7-8	$15'$-$16'$	15-16

Note that merging branches at leaf nodes, results in loss of information at those branch power losses. However, distribution networks are small in terms of area, meaning that the buses are close to each other. Hence, the losses in the system are assumed to be negligible compared to power demands where the loss of power loss information does not cause any problem.

3.3 Topology Mismatch Detection

After the system reduction procedure, topology mismatch can be detected. Topology mismatch detection method is based on WLAV SE. The weights of different types of measurements have to be determined first. The voltage magnitudes and current magnitudes are measured using only one instrument, the voltage transformer or the current transformer. However, power measurements are measured using both instruments, meaning that the inaccuracies of the instruments are combined in power mea-

surements. Hence, power measurement weights are less reliable than voltage magnitude and current magnitude measurements. Pseudo measurements that are based on forecasts have the lowest weight.

The proposed method cannot detect the precise location of topological mismatch but it can give an insight on the mismatch locations based on telemetered bus locations. The raw measurements gathered from the field and WLAV outputs are compared. There are two indicators for a topological mismatch. One indicator is based on power flow measurement signs. When the actual open switch is at a different subsection than the supposed one, the estimated power flow signs at the buses in between the actual and supposed subsection may be different than the raw power flow measurement sign. This leads to large residuals at these power flow measurements. The residuals of power flow measurements are tagged using Equation 3.1, if ϵ is more than 5. This value is decided empirically.

$$E_k = \left| \frac{r_k}{z_k} \right| \times 100 > \epsilon \quad k = 1 \dots m \tag{3.1}$$

Another indicator is the pseudo measurement residuals. Due to predefined measurement weight, the power flows may be kept the same by drastically increasing pseudo measurement residuals. By looking at the absolute value of residuals corresponding to pseudo measurements, it is possible to detect topological mismatches. It is observed that the 4 largest real power pseudo measurement residuals correspond to the non-telemetered observable buses that are at the ends of supposed and actual open switches. Only real power is considered as reactive power demand and generation at distribution level are low compared to real power which may mislead the results. Moreover, if the supposed open switch is at another subsection than the actual open switch, pseudo measurements at the edge of actual and supposed subsections change signs to minimize the objective function. Note that, if the supposed and actual open switches are on the two different branches of a ring, meaning that one of the edge nodes is common in the reduced network both supposed and actual network, the 3 largest pseudo measurements are checked.

In order to further clarify the procedure, consider the simple network given in Figure 3.7. Bus 0 indicated with green is the transmission system and is a teleme-

tered bus. Telemetered observable buses (5 and 11) are highlighted with blue, non-telemetered observable buses (1, 4, 6, 7, 10 and 12) are highlighted with red, and non-telemetered unobservable buses (2, 3, 8 and 9) are indicated with black. The dashed line between bus 6 and 12 indicates the supposed open switches. Assume that the actual open switches are on the branch between buses 3 and 4 which is indicated with a dashed line in Figure 3.8.

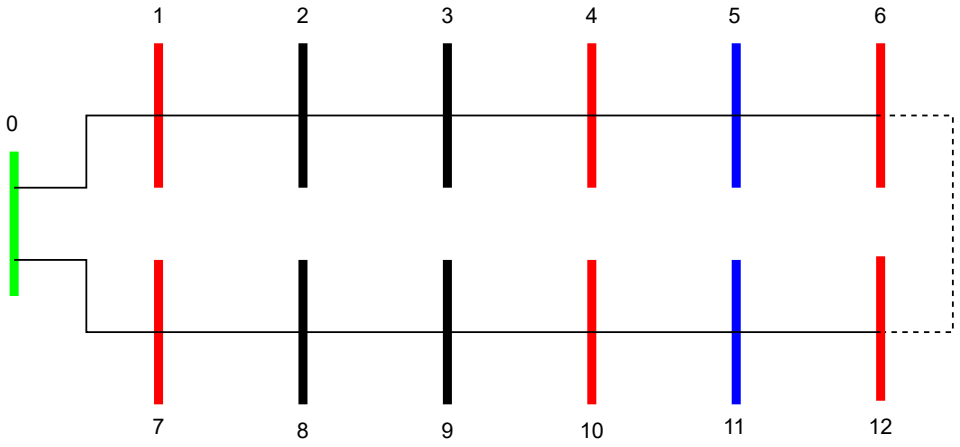

Figure 3.7: Supposed Topology of Example Network

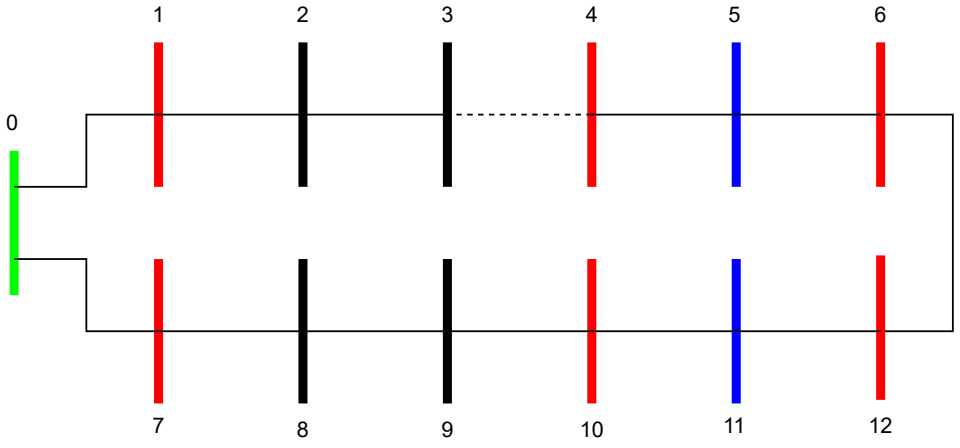

Figure 3.8: Actual Topology of Example Network

After reduction procedure in Section 3.2 is applied to both supposed and actual networks, Figure 3.9 and Figure 3.10 are obtained.

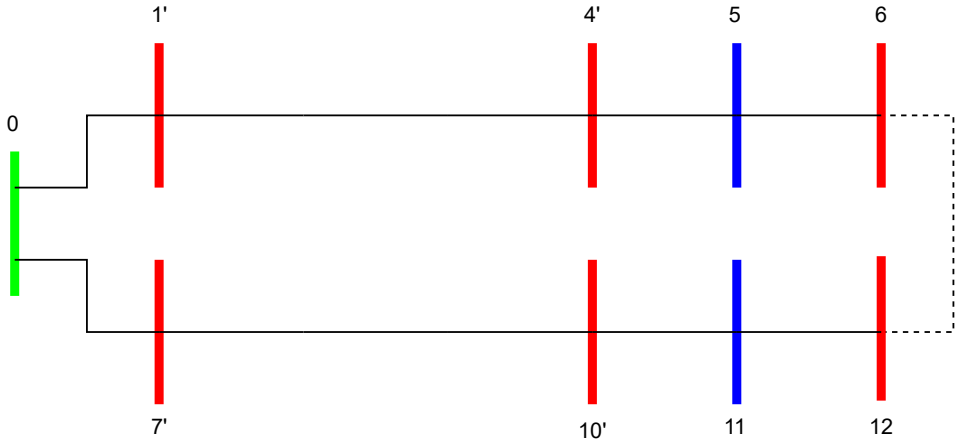

Figure 3.9: Reduced Topology of Supposed Example Network

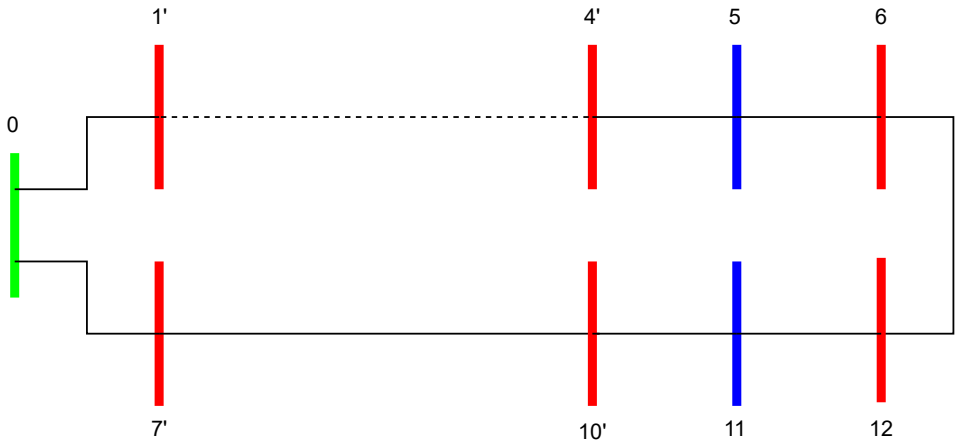

Figure 3.10: Reduced Actual Topology of Example Network

During implementation actual topology is not reduced as it is not known. It is only shown here to clarify the method. WLAV estimation is ran for the supposed system using the real-time measurements generated for the actual system. The estimator tries to minimize the residuals based on the supposed topology. Assume that the renewable energy sources at buses do not generate enough power so that the buses are active. Then in actual topology, real power is flowing from bus 5 to bus 4 is positive. However in supposed system, if every bus was demanding power, the power flowing from bus

5 to bus 4 would be negatively signed. So the estimator either changes the sign of power flow or changes the values of pseudo measurements at closest buses drastically to supposed and actual topology in order to minimize the objective function. The choice depends on the values of measurements and the adjusted weights for WLAV. The pseudo measurements of the closest buses are changed as the power flow between two pseudo measurements is not measured. So the amount of power those branches carry is not important in terms of SE as long as the residuals for the measurement set are minimized. Moreover, if the sign of power flow measurement is not changed, the sign of one pseudo measurement must change. In the given example, this bus is bus number 6. This bus must supply power so that the power flow from bus 6 to bus 5 and bus 5 to bus 4 can be positive.

Note that for the considered cases, the supposed and actual open switches are located between two different non-telemetered observable buses. Other cases are if the open switch is located at a branch that is measured by real-time measurements or one branch leads to an non-telemetered unobservable bus. Detection of topological errors at the first one is trivial as the branch is already measured by real-time measurements. However, topological error detection of the latter case is not possible as the only information inferred about those buses and branches are only based on pseudo-measurements.

Consider another case where a ring structure inside the supposed network is introduced as shown in Figure 3.11. Assume that the actual network is as in Figure 3.12. The color coding is the same as previous example. Telemetered observable buses are highlighted with blue while non-telemetered observable buses are highlighted with red. Bus 0 highlighted with green is the connection to transmission level. Black buses indicate the non telemetered unobservable buses.

The reduced systems for the supposed and actual networks can be observed in Figure 3.13 and Figure 3.14, respectively.

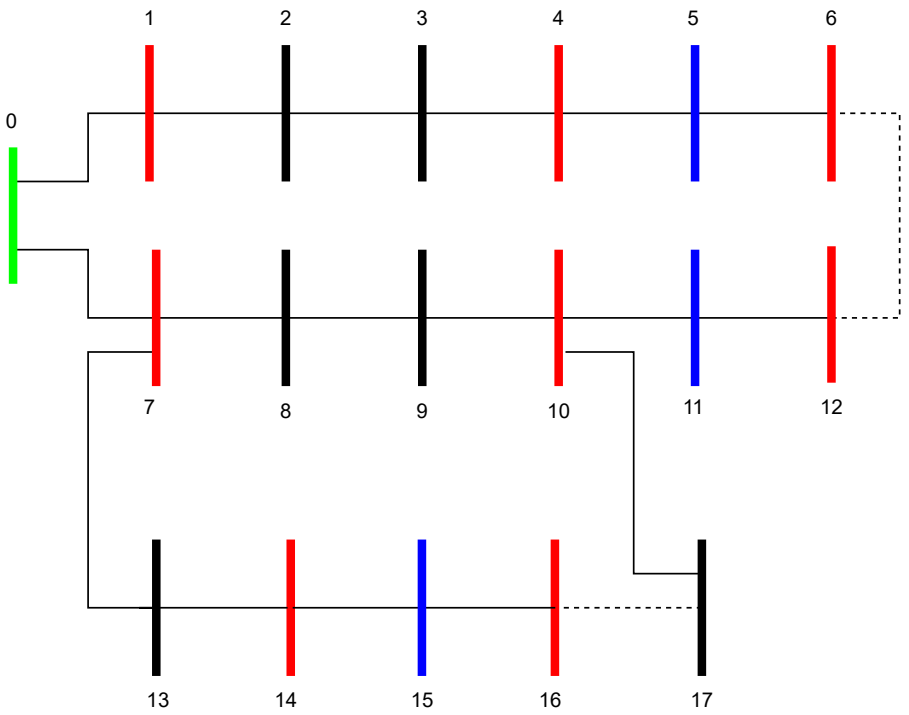

Figure 3.11: Supposed Network with Ring Structure

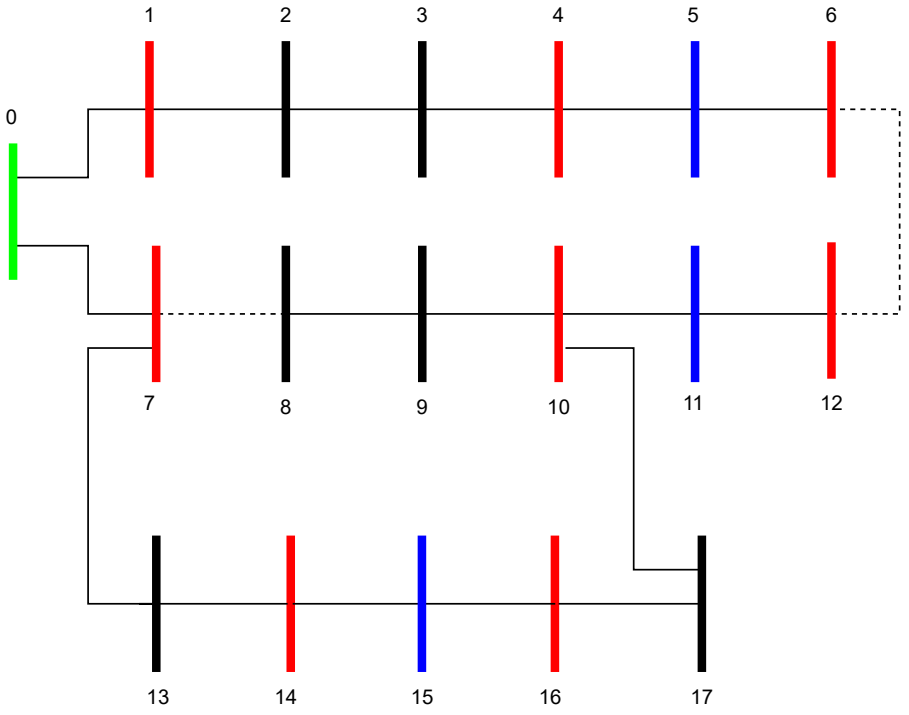

Figure 3.12: Actual Network with Ring Structure

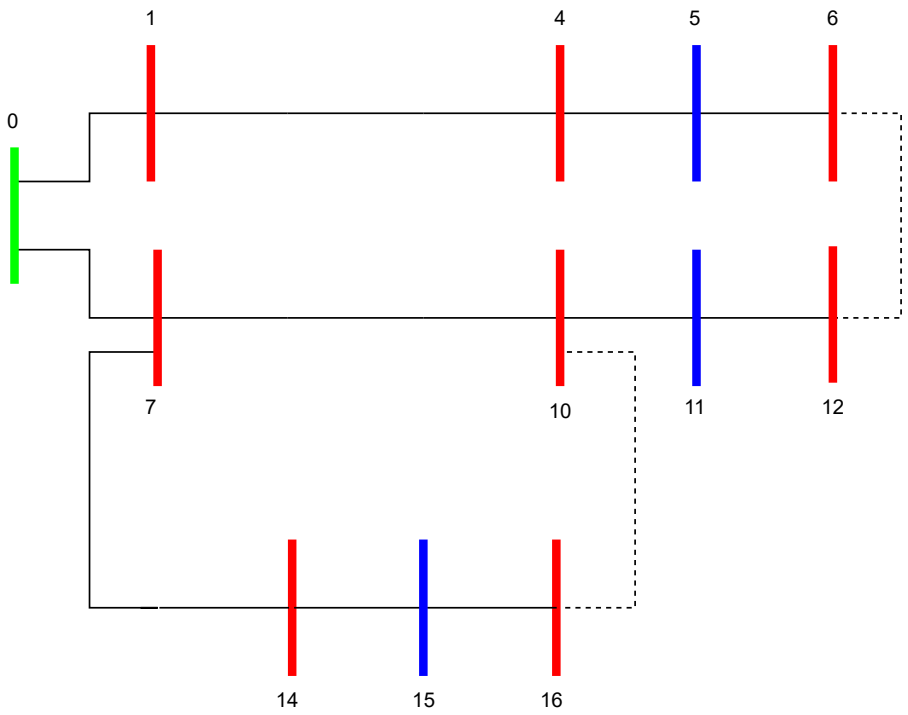

Figure 3.13: Supposed Network with Ring Structure after Reduction

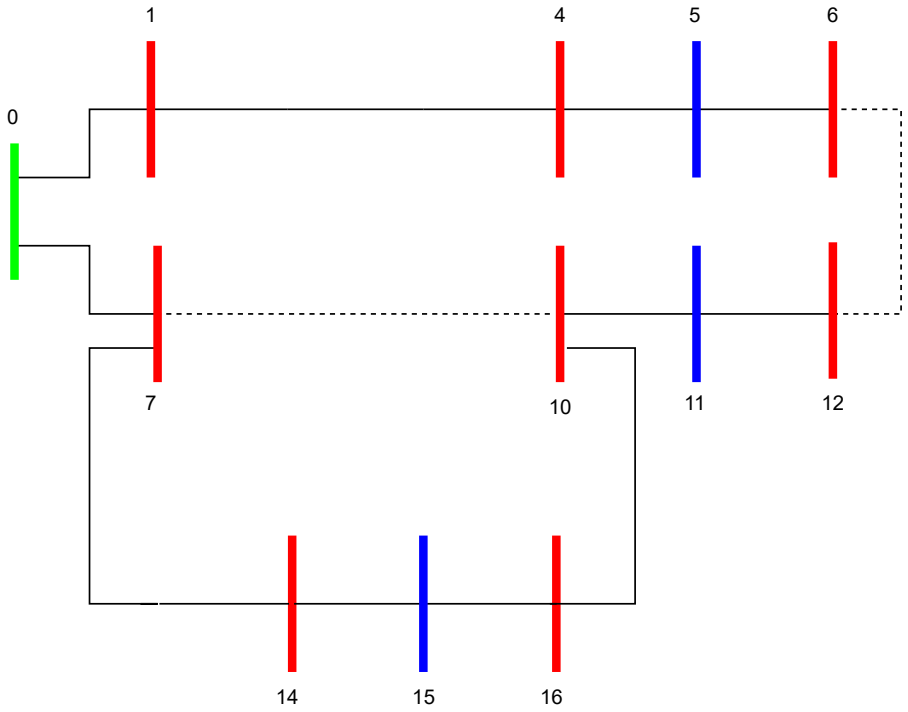

Figure 3.14: Actual Network with Ring Structure After Reduction

Real-time measurements are generated based on the actual topology given in Figure 3.12. In supposed network the real-time measurements at the top branch (0-1, 1-4, 4-5, 5-6) can be satisfied without increasing the residuals of any measurement as the actual and supposed networks overlap there. For the bottom side of the network, power flowing from bus 0 to 8 is the same except the the difference in open line losses. However, power flows at branch 14-15 and branch 15-16 change significantly between supposed and actual network. In actual network those branches carry the loads of bus 10,11 and 12 on addition to the loads they carry in supposed network. To reduce the objective function the estimator will again either try to change power flows or pseudo measurements based on measurement weights. Note that, when checking for largest pseudo measurements the largest 3 should be considered for such a case as bus 10 is common in both supposed (16-10) and actual open branch (6-10).

Flowchart of the proposed method is shown in Figure 3.15.

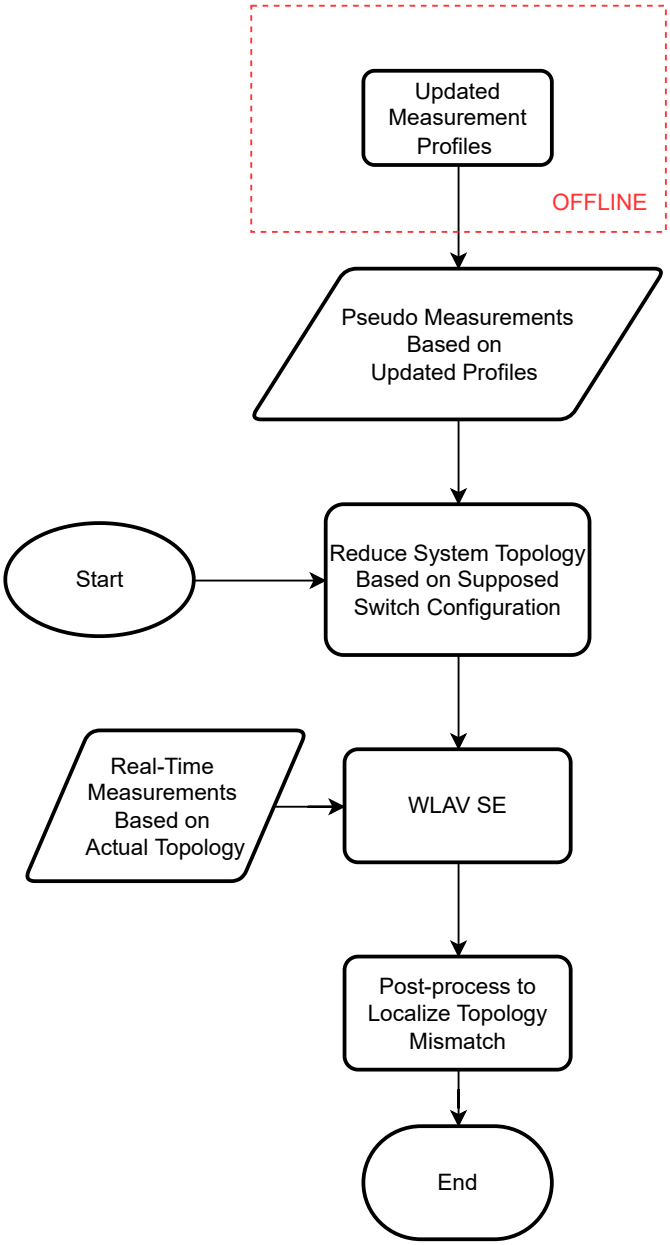

Figure 3.15: Proposed Method Flowchart

3.4 Chapter Summary

In this chapter, proposed method for topological mismatch detection is discussed in detail.

In Section 3.1, a method to update customer load profiles is explained. Customer load profiles have to be updated regularly to improve performance of analysis tools.

In Section 3.2, a system reduction algorithm to reduce the size of the system based on real-time measurement locations is explained. If the system is not reduced the high number of unreliable measurements bias the system. Moreover, since full system observability is achieved with pseudo measurements they become critical measurements. In this case, even if the measurements are inaccurate WLAV SE will try to minimize their residuals. By applying the system reduction method, pseudo measurements no longer bias the system.

In Section 3.3, a post-process procedure applied to WLAV SE results to identify topological mismatches is explained. There are two different cases to identify topological mismatches which are based on measurement residuals. Depending on measurement values and measurement weights assigned at WLAV, either power flows between the supposed and actual topology change sign or the pseudo measurements at closest buses change radically.

The method solves the problem of topological mismatch identification in power distribution systems with limited number of measurements. The limited number of measurements is compensated with pseudo measurements. The following assumptions are made for the proposed method:

- No bad-data is present in real-time measurements
- Measurement instruments are connected correctly.
- Large generations are measured and telemetered with real-time measurements.
- All buses are connected to the same feeder.
- The losses in the system are negligible compared to demands.

CHAPTER 4

RESULTS

The proposed method is tested on a power distribution network based on MV Oberrhein [24]. The network is shown as a ring structure in Figure 4.1 but it is operated radially under normal operating conditions. Every branch is assumed to be equipped with switches, meaning that every bus can be fed from at least two different branches.

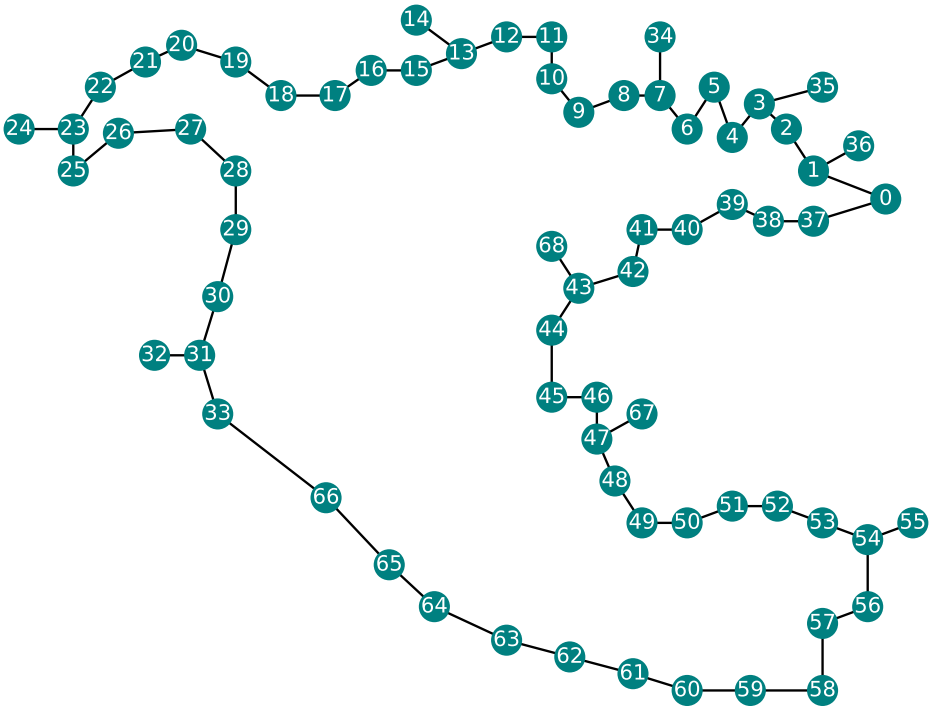

Figure 4.1: Network Generated Based on MV Oberrhein

The tests are done in Python 3.10 environment [25]. The example MV Oberrhein network is extracted from the PandaPower [24] library. Then, some of the system is removed to simplify test case generation. The created system is saved to be used in test cases. Examples for the test case file are shown in Appendix C Figure C.1 and Figure C.2.

The results for different steps of proposed method are given in the following subsections.

4.1 Profile Update

Real-time measurement and pseudo measurement data is generated using the open-source data obtained from Electricity Market Regulatory Authority (EMRA) [26]. The data consists hourly load demand of Turkey for each day of January 2022. The average of the first two weeks is used to create customer load profiles as the first two weeks were following the seasonal load demand trend.

In the following weeks, the industry slowed down due to natural gas shortage in Turkey, resulting in a decrease in electricity consumption. Those weeks are used to generate real-time measurements. The data obtained from EMRA and the load profile generated from the first two weeks can be observed in Figure 4.2 and Figure 4.3, respectively.

The proposed method assumes that the number of telemetered buses is limited for distribution networks. Hence, 10% of the buses are selected as telemetered buses which are highlighted in Figure 4.4 with red nodes. The green node is the connection with the transmission level and is also a telemetered bus. Moreover, the branch at bottom left of Figure 4.4 is not shown to indicate that the switches of that branch are open.

Using the data given in Figure 4.2, real-time measurements are generated for each hour of the month. To achieve system observability, pseudo measurements are introduced to the buses highlighted with blue in Figure 4.4. The real parts of pseudo measurements are generated using the data in Figure 4.3 and reactive parts are calcu-

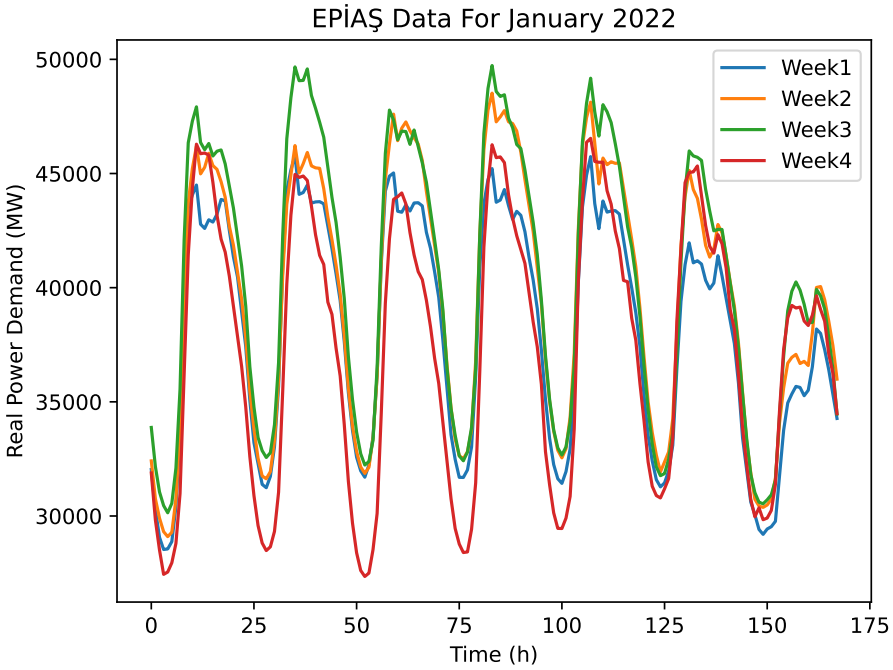

Figure 4.2: EMRA Data for Measurements

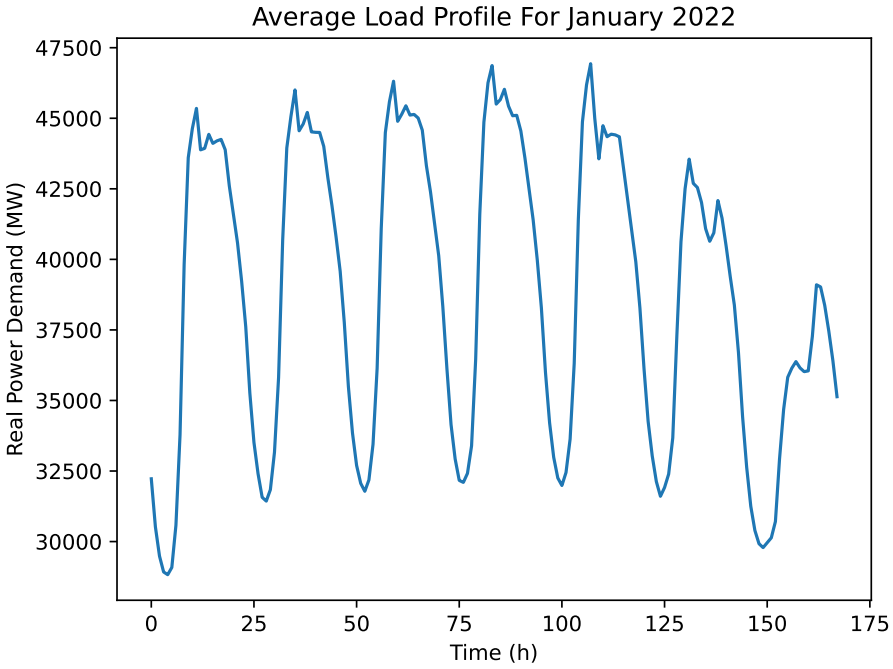

Figure 4.3: Generated Load Profile

lated by assuming the power factor as 0.9 lagging. The weights of the measurements are adjusted based on the measurement type.

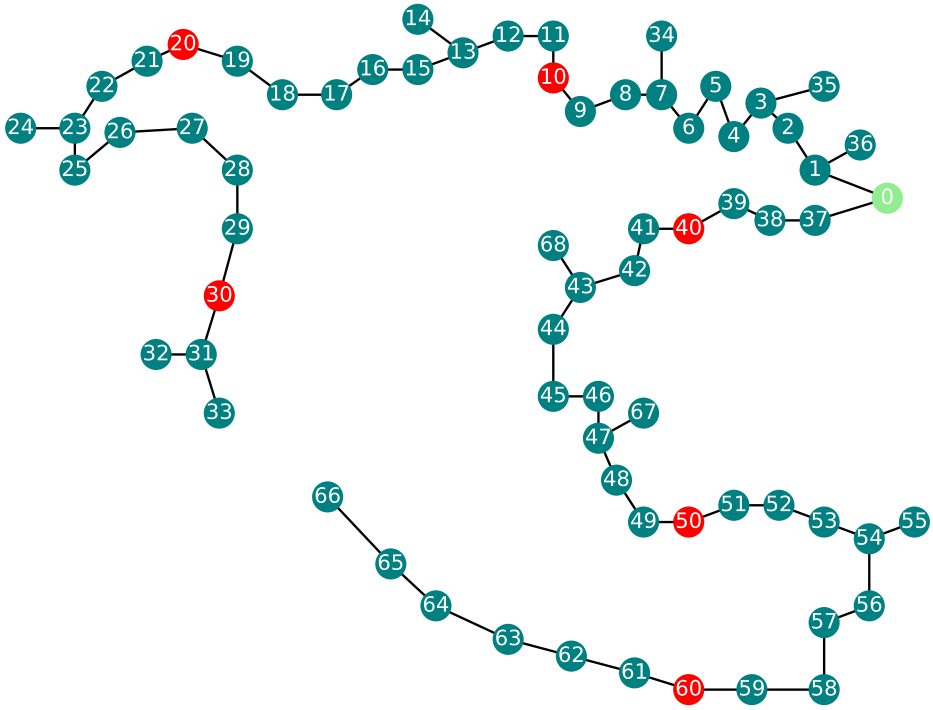

Figure 4.4: Network With Measurements Highlighted

Using the estimated states, the profiles are updated using Equation 2.14 and Equation 2.15. Since pseudo measurements bias the results, the update is done when there is a large difference between the estimated profile and the original profile. The result of pseudo measurement update can be observed in Figure 4.5.

With updated pseudo measurements given, system states are estimated again. The true states calculated using DLF, estimated states using out-of-date pseudo measurements and estimated states using updated pseudo measurements are shown in Figure 4.6 and Figure 4.7. It can be seen that voltage magnitudes and voltage angles when estimated with updated pseudo measurements are much closer to the true values when compared to estimation results with out-of-date pseudo measurements.

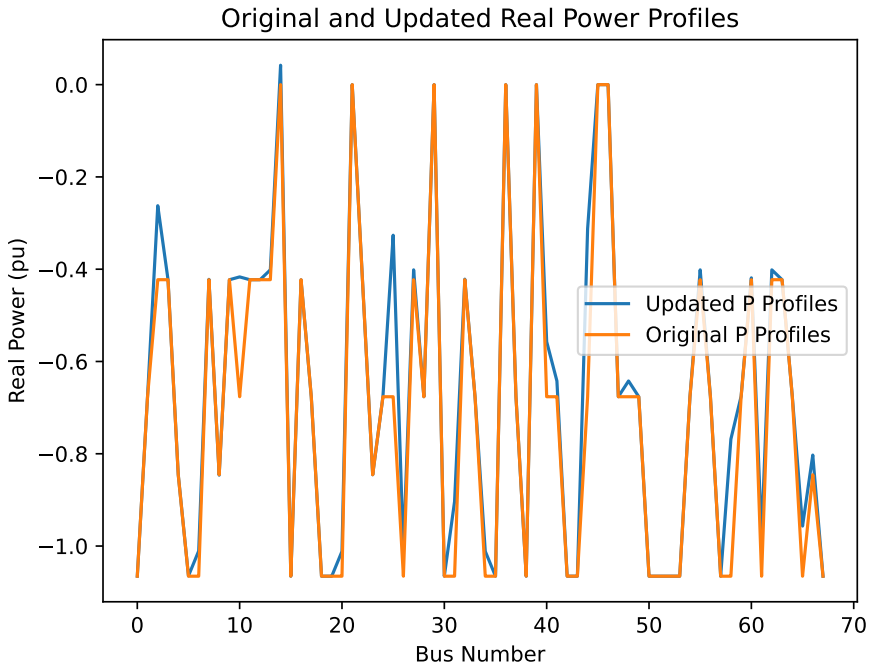

Figure 4.5: Updated and Original Real Power Injection Profiles

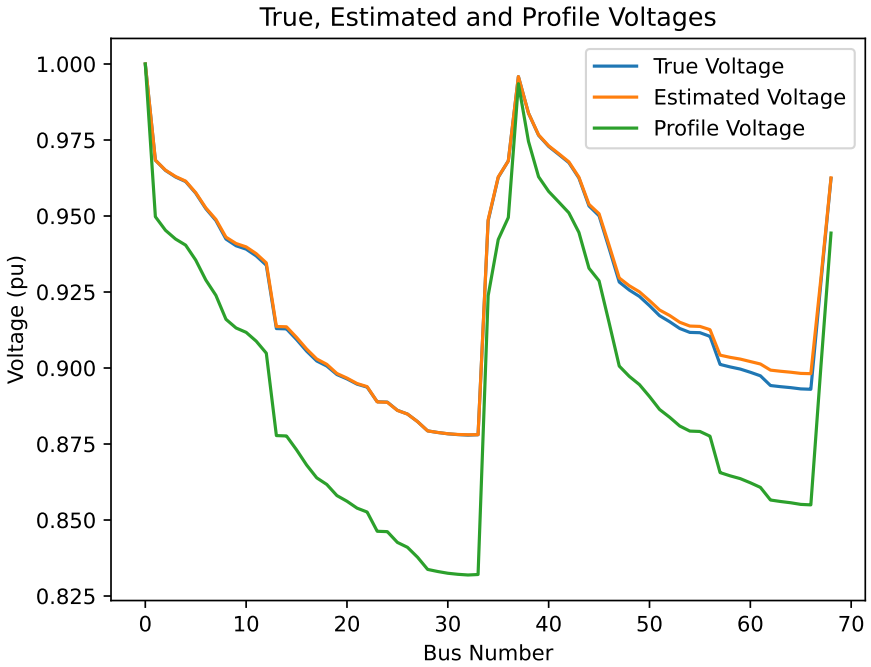

Figure 4.6: True, Estimated and Profile Voltages For a Single Time-Step.

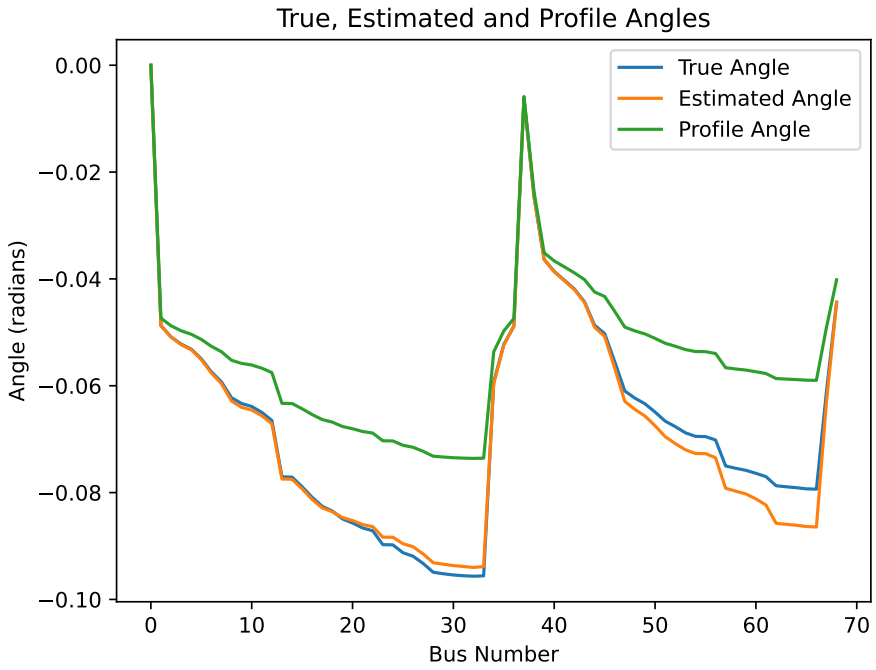

Figure 4.7: True, Estimated and Profile Angles For a Single-Time Step

The root mean square error (RMSE) and mean absolute error (MAE) values for voltage magnitudes and voltage angles are given in Table 4.1. It can be observed that updating the profiles has decreased both RMSE and MAE for both voltage magnitudes and voltage angles.

Table 4.1: Update Method Errors

State Name	**RMSE**	**MAE**
Estimated Voltage Magnitude with Updated Profiles	0.0183	0.0011
Estimated Voltage Magnitude with Out-of-Date Profiles	0.03236	0.03052
Estimated Voltage Angle with Updated Profiles	0.0263	0.00171
Estimated Voltage Angle with Out-of-Date Profiles	0.01439	0.01244

4.2 System Reduction

Now that the profiles are updated, it is possible to detect topological mismatches. The first step is to reduce the topology. Assume that the supposed and actual topology are as in Figure 4.4 and Figure 4.8, respectively.

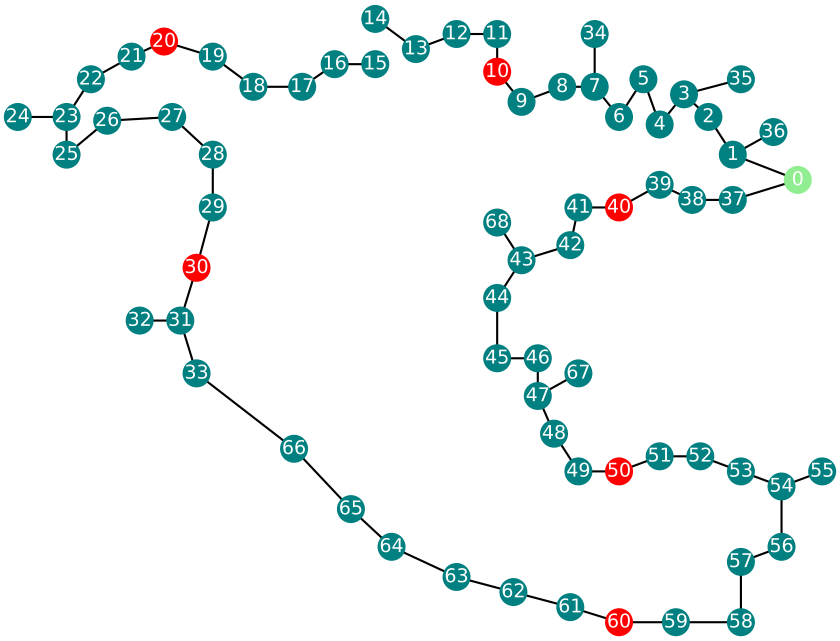

Figure 4.8: Actual Topology

The measurement configuration is the same as in Figure 4.4. The supposed system is reduced using the proposed method given in Section 3.2. First step is to merge radial connected leaf nodes until a non-telemetered observable bus or a bus with more than three branches connected is reached. The second step of reduction procedure is to merge non-telemetered unobservable buses that are not intersection to non-telemetered observable buses. The reduced network after steps 1 and 2 is given in Figure 4.9.

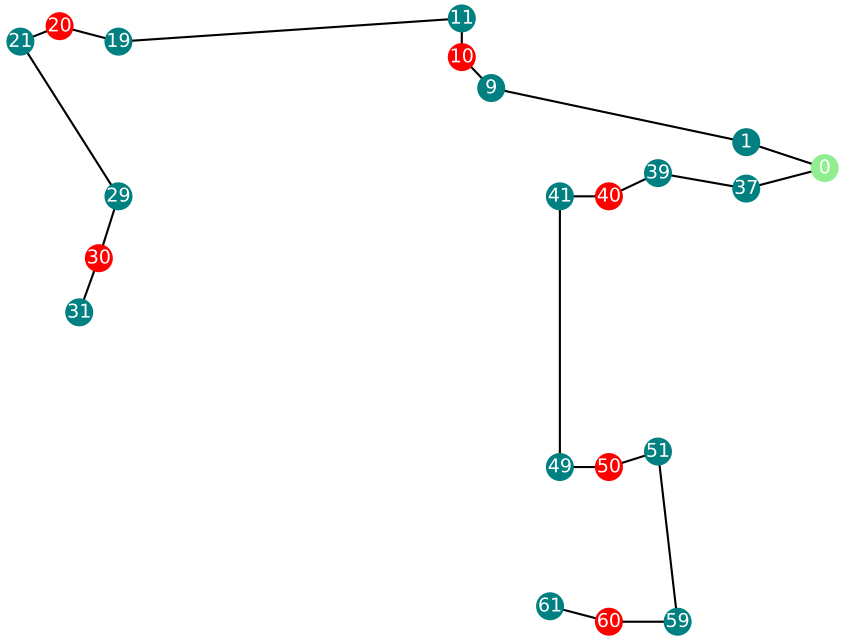

Figure 4.9: Reduced Network for MV Oberrhein

4.3 Topology Mismatch Detection

For the given case, topological errors are identified using WLAV SE. The supposed open switches are between buses 33 and 66 as can be seen in Figure 4.4. However, the actual open switches are located between buses 13 and 15 which can be observed in Figure 4.8. The mismatches are detected based on reduced system topology given in Figure 4.9.

True states are used to generate real-time measurements. Gaussian errors are added to real-time measurements based on measurement types. Measurements with higher reliability have lower variances and vice versa. It is assumed that real-time measurements do not carry bad data. Pseudo measurements are generated based on updated profiles given in Section 4.1. The WLAV SE is performed using the measurement set. The resulting residuals for WLAV SE are compared with the measurement set as explained in Section 3.3.

The results show that the highest 4 pseudo measurements residuals in the system correspond to buses 11, 19, 31 and 61. When checked in the reduced system given in Figure 4.9, it can be observed that these buses are the edges of the subsections that correspond to supposed and actual open switches. The results are also highlighted in Figure 4.10 in a reduced network, where the supposed open switch is highlighted with a green dashed line and the actual open switch is highlighted with a blue dashed line. 4 buses with largest pseudo-measurement residuals are also highlighted with red.

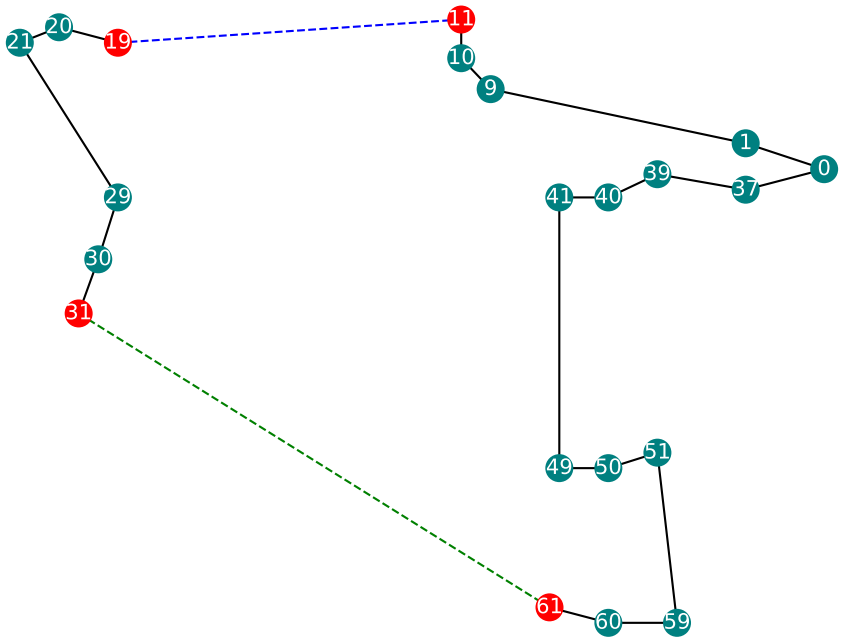

Figure 4.10: Highlighted Results for Case #1

More results are tabulated for different supposed and actual open switch combinations in Table 4.2, while some of them are also showed in Appendix B.

Table 4.2: Mismatch Detection Results

Case No	Supposed Open Switches	Actual Open Switch	Largest Residuals
1	33-66	13-15	11, 19, 31, 61
2	13-15	33-66	11, 19, 31, 61
3	13-15	43-44	11, 19, 41, 49
4	23-25	56-57	21, 29, 51, 59
5	16-17	63-64	11, 19, 41, 49
6	4-5	51-59	1, 9, 51, 59

The absolute values of pseudo measurement residuals are ordered from high to low as shown in Table 4.3 for the first case.

Table 4.3: First Case Residual Results

Pseudo Measurement	Absolute Value of Residual
11	35.477
19	32.307
61	5.032
31	4.976
49	1.532
41	1.473
59	1.121
1	1.109
9	1.109
29	0.824
51	0.82
21	0.617

As can be observed from Table 4.3, residuals of pseudo measurements at supposed and actual open branch edges are the largest 4 by a high margin.

Note that above examples does not account for the ring structures in the network.

Consider the modified network with a ring structure given in Figure 4.11, where 4 new buses (69, 70, 71 and 72) are introduced between bus 38 and bus 67.

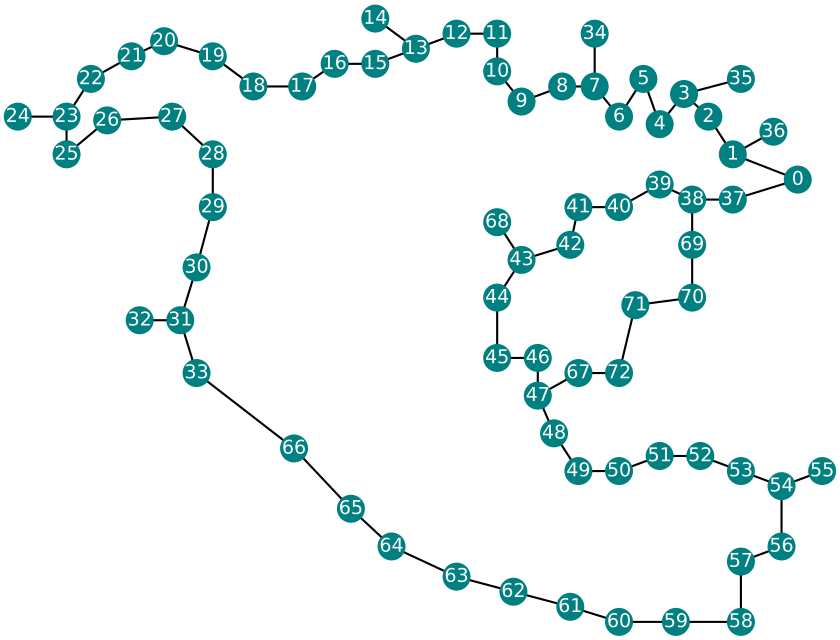

Figure 4.11: Modified Network with Ring Structure

Measurement redundancy is the same where 10% of the buses are telemetered buses. The measurement configuration is shown in Figure 4.12, where red buses indicate telemetered buses.

Assume that the switches between bus 45 and bus 46 is are supposed to be open. However in reality, switches between buses 67 and 72 are open. Of course for system to be radially operated another set of switches should be open. Assume that the switch at the branch between buses 33 and 66 are open both in supposed and actual network. The reduced network for the supposed system can be observed in Figure 4.13 and the results of the detection procedure are highlighted in Figure 4.14. Supposed open switch is highlighted with green dashed line and the actual open switch is highlighted with blue dashed line. Largest pseudo measurements are also highlighted with red. Note that in this case since bus 49 is common for both actual open switch and the supposed open switch, largest 3 residuals are considered for localization of topological mismatch.

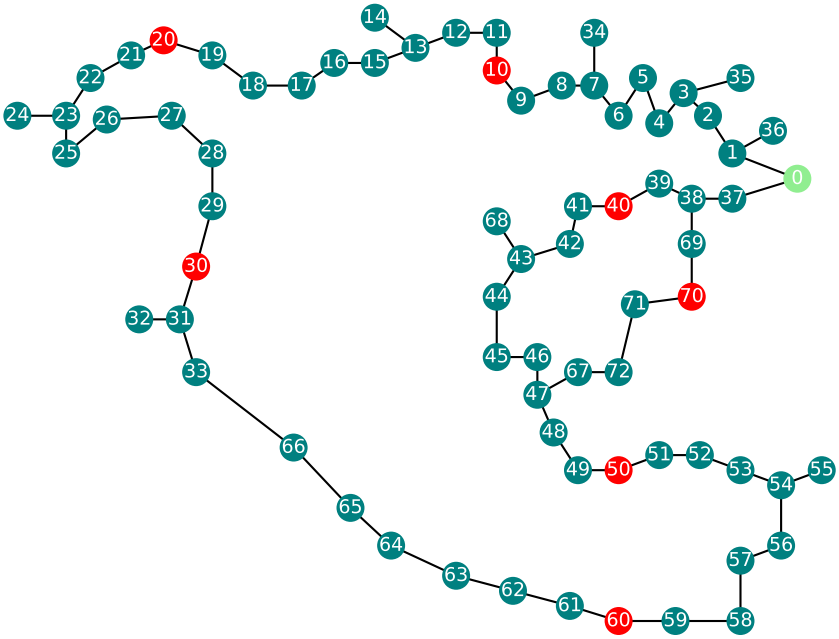

Figure 4.12: Measurement Configuration of Modified Network with Ring Structure

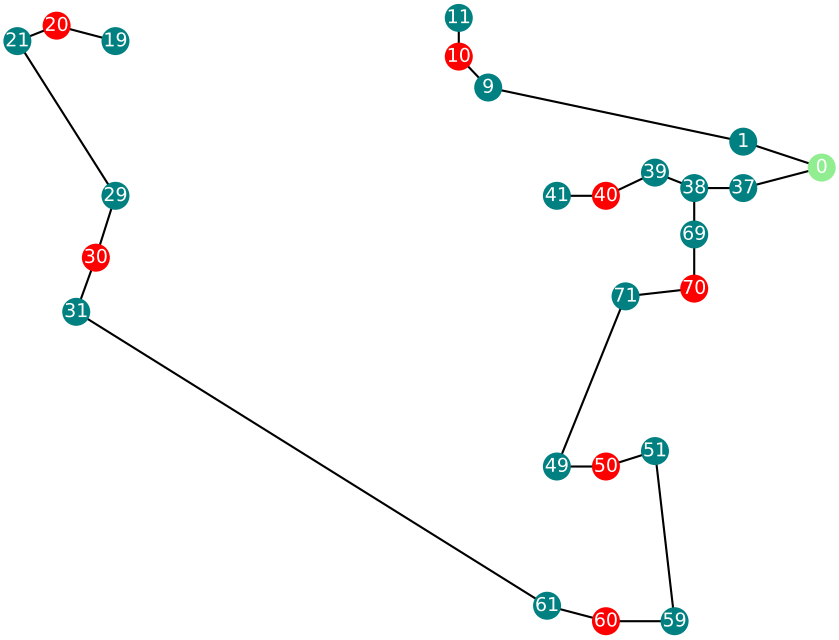

Figure 4.13: Reduced Network for Modified Network with Small Ring

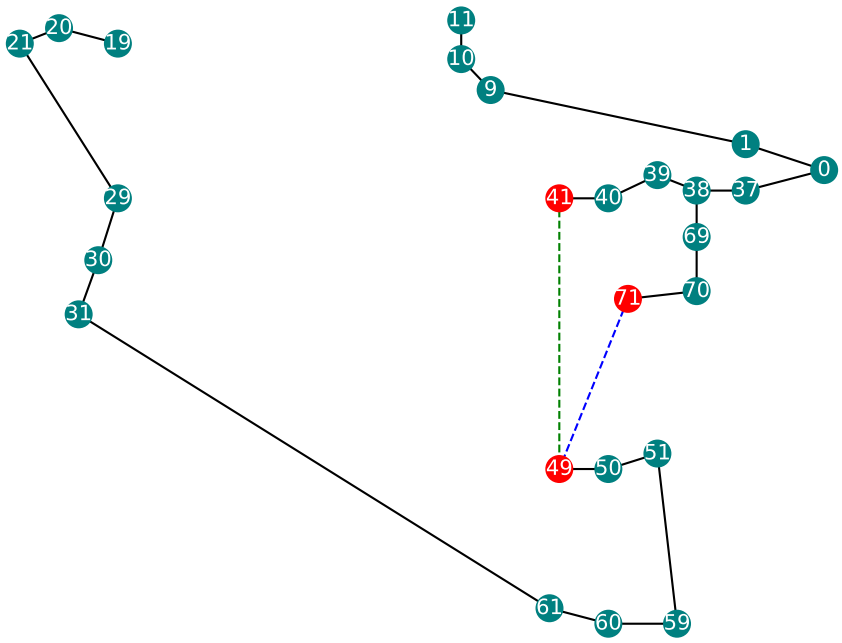

Figure 4.14: Result for Modified Network with Small Ring

Last case considered is when there are multiple connections to transmission level in the network. This case is similar to the base cases. A new bus namely 69 is added to the base system. Assume that in supposed network open branches are 33-66 and 53-54, while in actual network switches at branches 33-66 and 46-47 are open. The supposed and actual networks can be observed in Figure 4.15 and Figure 4.16, respectively.

When the proposed method is applied to the network, pseudo measurements at buses 51, 59, 41 and 49 are found to be the erroneous ones. This corresponds to the supposed and open switches. The results for topology identification method for multiple feeder case are also highlighted in Figure 4.17.

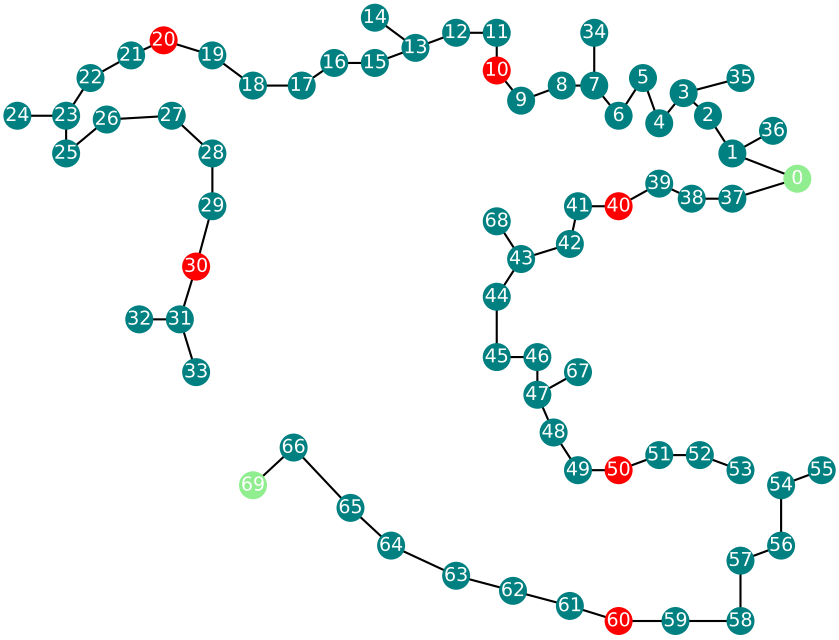

Figure 4.15: Supposed Network for Multiple Feeder Case

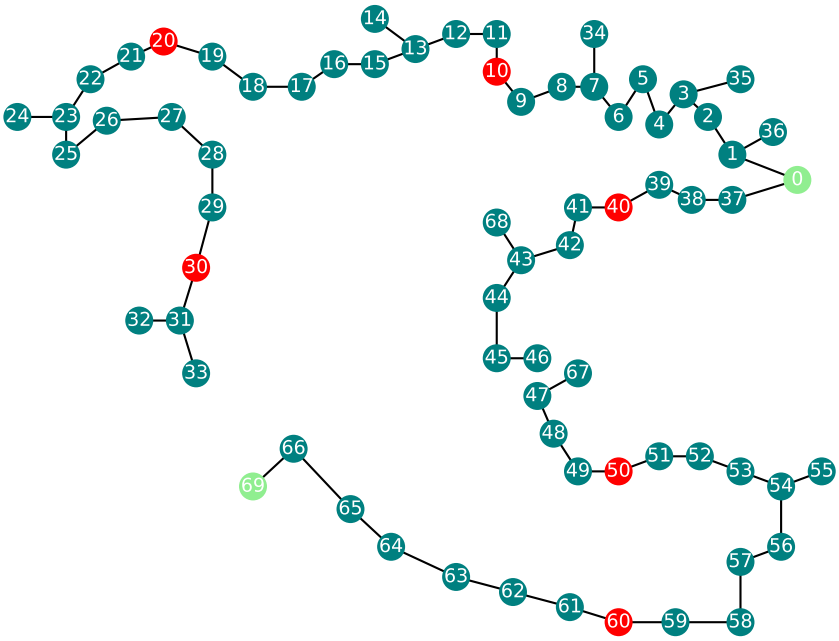

Figure 4.16: Actual Network for Multiple Feeder Case

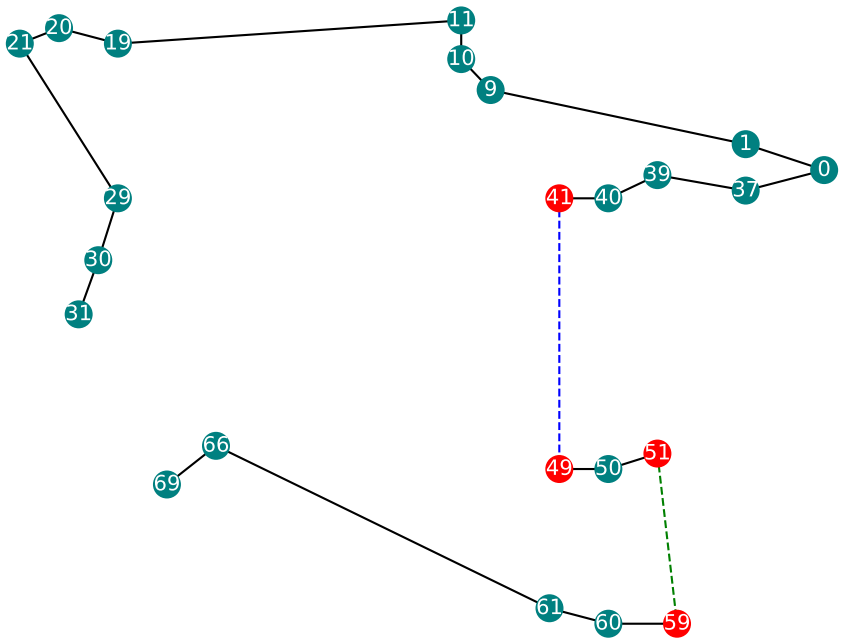

Figure 4.17: Results for Multiple Feeder Case

4.4 Chapter Summary

In this chapter, the proposed method is applied to a test network MV Oberrhein. The load data is gathered from EMRA [26].

In Section 4.1, the customer load profiles are generated based on gathered data. The results show that the update of customer load profiles is crucial for systems that pseudo measurements are actively used. Distribution systems with limited measurements is an example of such systems.

In Section 4.2, the reduction method is applied to the MV Oberrhein network. The results show that the applied methodology is correct for different topological configurations as the system is reduced as intended. By reducing the system pseudo measurements are no longer critical measurements.

In Section 4.3, WLAV SE is applied for the reduced network generated in Section 4.2. The results are highlighted in several network graphs and also tabulated. Then, the

network is extended to contain small rings. It is observed that the method also gives desired results for networks with small rings.

To conclude the chapter, results show that using WLAV SE it is possible to detect topological mismatches in distribution systems with limited number of measurements. The topological mismatches were detected accurately, where in this thesis only a portion of all cases are given.

CHAPTER 5

CONCLUSION

In this thesis, a method to detect topological mismatches in power distribution systems with limited number of measurements is developed. The developed method relies on two tools which are DLF and WLAV SE. DLF is an application of FBPF. It offers better performance than the conventional FBPF as the system is only traced once in DLF while in FBPF the system is traced in each iteration. WLAV SE is an extension of the well-known LAV SE, where measurements can also be weighted depending on their reliability. In distribution networks there are limited number of measurements. To compensate for lact of measurements and obtain full system observability, pseudo measurements are introduced to state estimation algorithm.

The developed method can be divided into three parts. First part is the customer load profile update. Load profiles are updated based on WLAV results to improve performance of further analysis tools such as DLF or WLAV. Second, a system reduction method is employed to improve the performance of WLAV SE in power distribution networks with limited number of real-time measurements. The reduction is done based on real-time measurement locations. Lastly, the results of WLAV SE are post-processed to localize topological mismatches based on measurement locations.

The customer load profile update method utilizes WLAV results. This method is employed when the correct topology of the system is known. The profiles are updated only when there is a large mismatch between the updated profile and the original profile. The performance update is validated using DLF. Results of updated profiles are much closer and have smaller RMSE and MAE values when compared to results of original profiles.

Full system observability is achieved by pseudo-measurements in power distribution systems with limited measurements. These measurements are generated from the updated load profiles and generation forecasts. Most of the buses do not have real-time measurements, meaning that the number of pseudo-measurements is large compared to real-time measurements. A novel system reduction method is employed to reduce the number of pseudo-measurements as most of them are critical measurements that would bias WLAV results.

Topology mismatches are detected in a post-process where the signs and values of power flows and pseudo-measurements are checked. Depending on the post-process results, the topological mismatches are located on subsection level. The subsections are defined based on measurement locations.

To sum up, profile update method improves the performance of analysis tools. The updated profiles are used in the topological mismatch detection method where a system reduction algorithm is employed to reduce bias in WLAV.

As future work, the current method can be expanded to include PMUs. They are not considered in this thesis since currently, PMUs are not commonly used in power distribution systems. Lastly, improvements can be made in computational performance of all tools utilized. Since, performance is not the main aim of the thesis sparse data structures and other tools to enhance computational performance are not utilized.

REFERENCES

[1] N. L. Panwar, S. C. Kaushik, and S. Kothari, "Role of renewable energy sources in environmental protection: A review," 4 2011.

[2] A. G. Olabi and M. A. Abdelkareem, "Renewable energy and climate change," *Renewable and Sustainable Energy Reviews*, vol. 158, 4 2022.

[3] G. Cavraro, A. Bernstein, V. Kekatos, and Y. Zhang, "Real-time identifiability of power distribution network topologies with limited monitoring," *IEEE Control Systems Letters*, vol. 4, pp. 325–330, 4 2020.

[4] R. L. Lugtu, D. F. Hackett, K. C. Liu, and D. D. Might, "Power system state estimation: Detection of topological errors," *IEEE Transactions on Power Apparatus and Systems*, vol. PAS-99, pp. 2406–2412, 1980.

[5] K. A. Clements, "Topology error identification using normalized lagrange multipliers," *IEEE Transactions on Power Systems*, vol. 13, pp. 347–353, 1998.

[6] E. Caro, A. J. Conejo, and A. Abur, "Breaker status identification," *IEEE Transactions on Power Systems*, vol. 25, pp. 694–702, 5 2010.

[7] F. F. Wu and E. L. Wen-Hsiung, "Detection of topology errors by state estimation," *IEEE Transactions on Power Systems*, vol. 4, pp. 176–183, 1989.

[8] A. Abur, M. Çelik, and H. Kim, "Identifying the unknown circuit breaker statuses in power networks," *IEEE Transactions on Power Systems*, vol. 10, pp. 2029–2037, 1995.

[9] M. E. Baran, J. Jung, and T. E. McDermott, "Topology error identification using branch current state estimation for distribution systems," 12 2009.

[10] Y. Gao, W. Wu, Z. Zhang, and H. Liang, *A Method for the Topology Identification of Distribution System*.

[11] M. Farajollahi, A. Shahsavari, and H. Mohsenian-Rad, "Topology identification in distribution systems using line current sensors: An milp approach," *IEEE Transactions on Smart Grid*, vol. 11, pp. 1159–1170, 3 2020.

[12] J. Zhang, Y. Wang, Y. Weng, and N. Zhang, "Topology identification and line parameter estimation for non-pmu distribution network: A numerical method," *IEEE Transactions on Smart Grid*, vol. 11, pp. 4440–4453, 9 2020.

[13] J. Zhao, L. Li, Z. Xu, X. Wang, H. Wang, and X. Shao, "Full-scale distribution system topology identification using markov random field," *IEEE Transactions on Smart Grid*, vol. 11, pp. 4714–4726, 11 2020.

[14] A. Bergen and V. Vittal, "Power systems analysis,"

[15] J. Ranjith Kumar R and A. Jain, "Load flow methods in distribution systems with dispersed generations: A brief review," *2015 1st Conference on Power, Dielectric and Energy Management at NERIST, ICPDEN 2015*, 04 2015.

[16] S. Chatterjee and S. Mandal, "A novel comparison of gauss-seidel and newton-raphson methods for load flow analysis," pp. 1–7, 03 2017.

[17] M. Srinivas, "Distribution load flows : A brief review," 2000.

[18] R. Berg, E. S. Hawkins, and W. W. Pleines, "Mechanized calculation of unbalanced load flow on radial distribution circuits."

[19] J. H. Teng, "A direct approach for distribution system load flow solutions," *IEEE Transactions on Power Delivery*, vol. 18, pp. 882–887, 7 2003.

[20] F. C. Schweppe and J. Wildes, "Power system static-state estimation, part i: Exact model," 1970.

[21] F. C. Schweppe and D. B. Rom, "Power system static-state estimation, part ii: Approximate model," 1970.

[22] F. C. Schweppe and D. B. Rom, "Schweppe: System static-state estimation, iii," 1970.

[23] A. Abur and A. G. Exposito, *Power system state estimation : theory and implementation*. Marcel Dekker, 2004.

[24] L. Thurner, A. Scheidler, F. Schäfer, J. Menke, J. Dollichon, F. Meier, S. Meinecke, and M. Braun, "pandapower — an open-source python tool for convenient modeling, analysis, and optimization of electric power systems," *IEEE Transactions on Power Systems*, vol. 33, pp. 6510–6521, Nov 2018.

[25] G. Van Rossum and F. L. Drake, *Python 3 Reference Manual*. Scotts Valley, CA: CreateSpace, 2009.

[26] EMRA, "Gerçek zamanlı tüketim." `https://seffaflik.epias.com.tr/transparency/tuketim/gerceklesen-tuketim/gercek-zamanli-tuketim.xhtml`, 2022. [Online; accessed 14-March-2022].

APPENDIX A

ALGORITHMS

Algorithm 1 Direct Load Flow Algorithm

1: Form **BIBC** Matrix
2: Form **BCBV** Matrix
3: Determine initial solution, $\mathbf{V_{bus}[0]}$
4: Calculate initial complex power injections at buses, $\mathbf{S_{bus}[0]}$
5: Determine threshold value, ϵ
6: **k** $\leftarrow 0,$ **error** $\leftarrow 100$
7: **while** $\max|\mathbf{error}| > \epsilon$ **do**
8: $\quad \mathbf{I_{bus}[k]} = \left(\frac{S_{bus}}{V_{bus}[k]}^{*}\right)$
9: $\quad \mathbf{I_{branch}[k]} = \mathbf{BIBC} \times \mathbf{I_{bus}[k]}$
10: $\quad \mathbf{V_{bus}[k+1]} = \mathbf{V_{bus}[k]} - \mathbf{BCBV} \times \mathbf{I_{branch}[k]}$
11: $\quad \mathbf{error} = \mathbf{V_{bus}[k+1]} - \mathbf{V_{bus}[k]}$
12: $\quad$ k = k+1
13: **end while**
14: bus voltage vector $\leftarrow V_{\text{bus}}[k+1]$

Algorithm 2 Weighted Least Absolute Value State Estimation Algorithm

1: Form bus admittance matrix, $\mathbf{V_{bus}[0]}$

2: Form measurement matrix, $\mathbf{z}$

3: Determine initial solution, $\mathbf{x^0}$

4: Determine threshold value, ϵ

5: $\mathbf{k} \leftarrow 0,\ \Delta x^0 \leftarrow 100$

6: **while** $\max|\Delta x^k| > \epsilon$ **do**

7: $\quad h[k] \leftarrow form.h(x^k)$

8: $\quad H \leftarrow form.H(x^k)$

9: $\quad C^T \leftarrow \begin{bmatrix} 0_n & 0_n & c_m & c_m \end{bmatrix}$

10: $\quad A \leftarrow \begin{bmatrix} H & -H & I_m & I_m \end{bmatrix}$

11: $\quad b \leftarrow z - h[k]$

12: $\quad \Delta x^k \leftarrow simplex.solver(C, A, b)$

13: $\quad x^{k+1} \leftarrow x^k + \Delta x^k$

14: $\quad k \leftarrow k + 1$

15: **end while**

16: estimated states $\leftarrow x^{k+1}$

APPENDIX B

ADDITIONAL HIGHLIGHTED RESULT GRAPHS

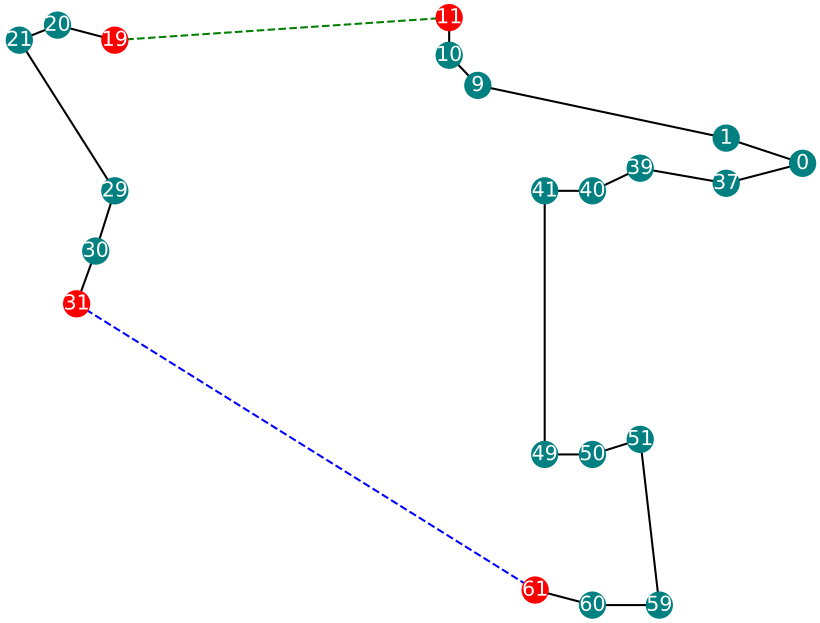

Figure B.1: Highlighted Results for Case #2

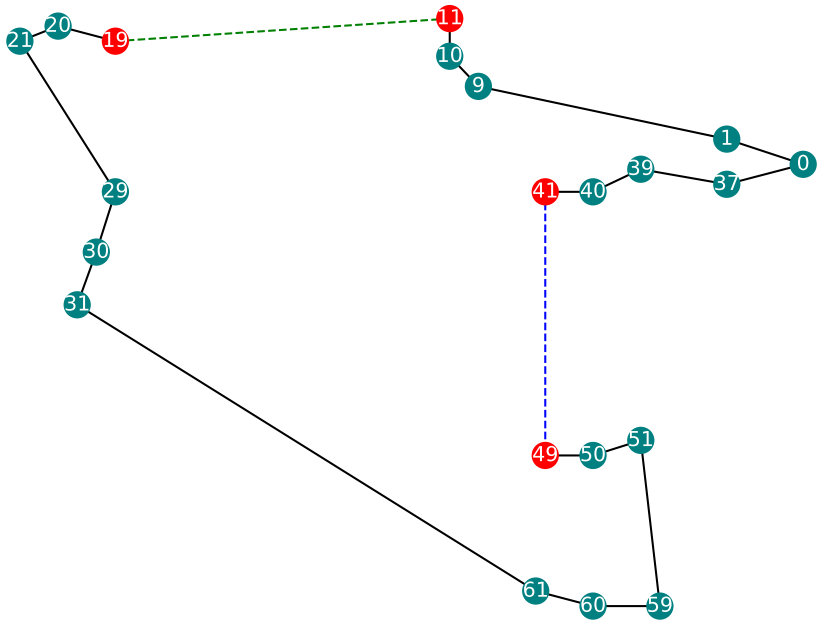

Figure B.2: Highlighted Results for Case #3

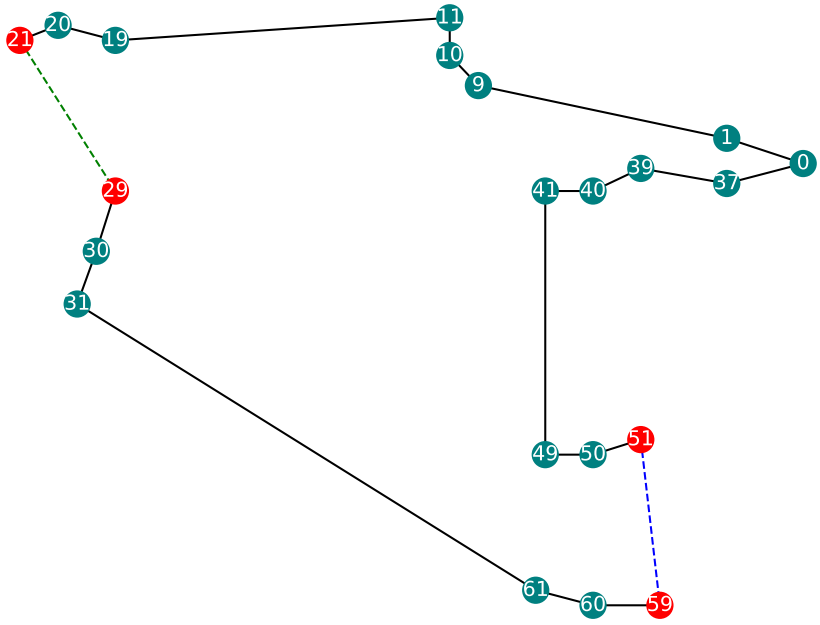

Figure B.3: Highlighted Results for Case #4

APPENDIX C

INPUT FILE EXAMPLES

	bus	pLoad	qLoad	pGen	qGen	x	y
0	0	0	0	0	0	3420200	5369365
1	1	0.378	0.076756	0	0	3419400	5369700
2	2	0.24	0.048734	0	0	3419100	5370200
3	3	0.15	0.030459	0	0	3418800	5370500
4	4	0.15	0.030459	0	0	3418500	5370100
5	5	0.3	0.060918	0	0	3418300	5370700

Figure C.1: Bus Data Example

	fromBus	toBus	resistancePU	reactancePU	totalSusceptancePU
0	27	28	0.00067934	0.000493682	0.05790199
1	26	27	0.000431722	0.000313736	0.036796821
2	31	32	0.000130209	9.46238E-05	0.011098053
3	19	20	0.000124292	0.000090324	0.010593752
4	18	19	0.000217892	0.000158344	0.018571562
5	13	14	0.000189256	0.000137534	0.016130771

Figure C.2: Branch Data Example